

---

# StableMTL: Repurposing Latent Diffusion Models for Multi-Task Learning from Partially Annotated Synthetic Datasets

---

Anh-Quan Cao<sup>1</sup> Ivan Lopes<sup>2</sup> Raoul de Charette<sup>2</sup>

<sup>1</sup>Valeo.ai <sup>2</sup>Inria

<https://github.com/astra-vision/StableMTL>

## Abstract

Multi-task learning for dense prediction is limited by the need for extensive annotation for every task, though recent works have explored training with partial task labels. Leveraging the generalization power of diffusion models, we extend the partial learning setup to a zero-shot setting, training a multi-task model on multiple synthetic datasets, each labeled for only a subset of tasks. Our method, StableMTL, repurposes image generators for latent regression. Adapting a denoising framework with task encoding, task conditioning and a tailored training scheme. Instead of per-task losses requiring careful balancing, a unified latent loss is adopted, enabling seamless scaling to more tasks. To encourage inter-task synergy, we introduce a multi-stream model with a task-attention mechanism that converts N-to-N task interactions into efficient 1-to-N attention, promoting effective cross-task sharing. StableMTL outperforms baselines on 7 tasks across 8 benchmarks.

## 1 Introduction

For many real-world applications, multi-task learning (MTL) offers a vital alternative to classical single-task models since MTL allows solving multiple tasks at once. This is of utmost importance for computer vision systems interacting with our world such as robotics or virtual reality which typically require estimating various scene cues (*e.g.*, semantic segmentation, depth, optical flow, etc.) in a time-sensitive manner. Beyond practical aspects, a vast body of literature shows that different tasks learn at least partially distinct representations that can benefit other tasks [74, 54]. Because it learns multiple tasks at once, MTL offers an ideal setting to enforce information exchange across tasks [57]. However, the benefits of MTL is impeded by the small number of datasets with multiple overlapping task labels, especially for dense predictions given the cost of pixel-level annotation [46].

An alternative is to train in a partially labeled setup [32] – that is, using images with annotations for a subset of all tasks. This differs from prior semi-supervised setting [47, 21] which typically overlooks the crucial inter-task relationships. Yet, existing partially annotated MTL methods [32, 71, 46] are confined to training on a single domain, therefore offering poor generalization capability, and struggling to balance conflicting task objectives [57].

To reduce reliance on extensive annotations, we propose a new setting, leveraging *multiple synthetic datasets* with partial labels. This, however, introduces a synthetic-to-real domain gap, necessitating models with strong generalization capability to real-world data. We address this by building upon recent findings that pre-trained Latent Diffusion Models (LDMs), originally designed for image generation, can be repurposed for dense prediction tasks [27, 25, 40, 66] by preserving the LDM’s rich latent space while fine-tuning only the UNet. In fact, such models exhibit remarkable real-world generalization, even when trained on relatively small synthetic datasets.

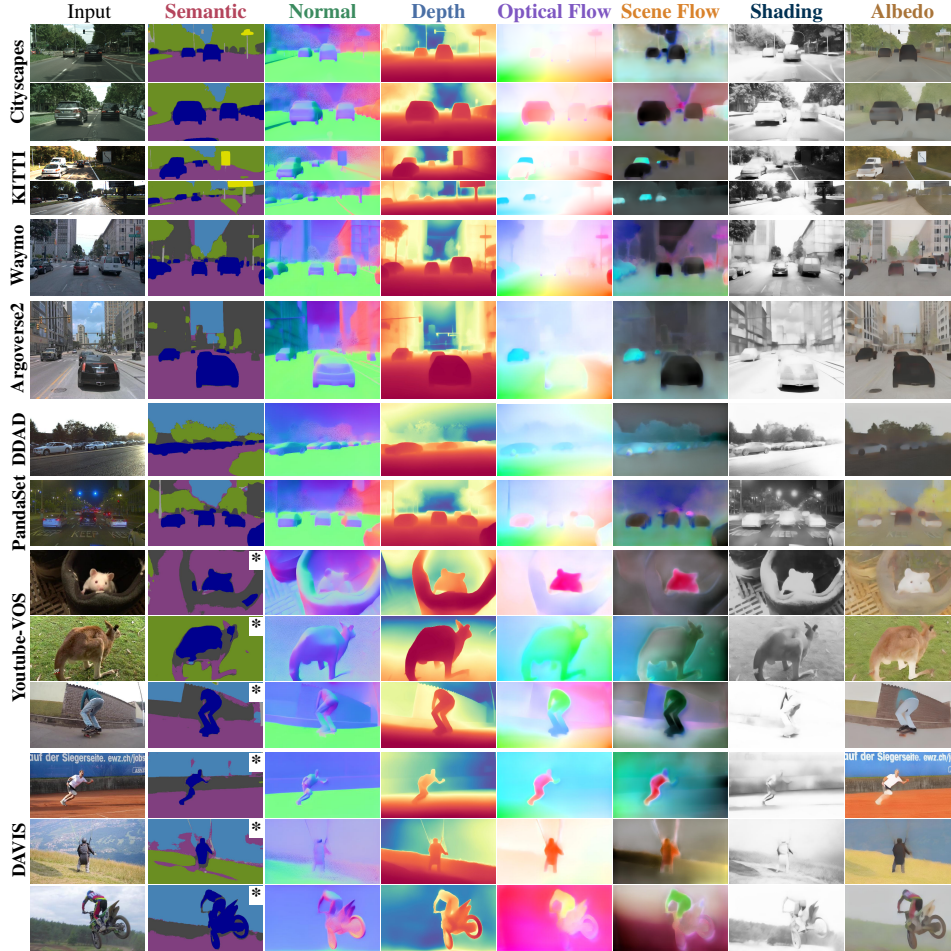


Figure 1: **StableMTL output on unseen real-world data.** StableMTL demonstrates robust generalization to real-world data, despite being trained on partially labeled synthetic datasets. \* Note that **semantic** is trained on driving classes and is not expected to generalize to unseen classes.

In practice, our method StableMTL, extends deterministic single-step LDMs [25] to the partially labeled multi-task setting with task-token conditioning. Additionally we make use of a custom training scheme that decouples task-specific gradients. To benefit from cross-task interactions, rather than N-to-N attentions [37, 7], which scales poorly to higher number of tasks, our multi-stream architecture enables a more efficient N-to-1 task inter-task attention mechanism. While adding tasks typically necessitates specific losses, our approach eliminates this requirement by unifying them into a single and simple latent Mean Squared Error (MSE) loss, thereby significantly enhancing scalability. In summary, our methodological contributions are twofold:

- We introduce a more realistic partially labeled MTL setting, training on multiple synthetic datasets, each with partial task annotations.
- Our method, StableMTL, repurposes pre-trained image generation Latent Diffusion Models for MTL, using a multi-stream architecture favoring task exchanges via N-to-1 attention. By employing a single, unified latent loss across all tasks alongside a tailored training scheme, our method eliminates the need for task-specific losses and complex inter-task balancing.

As shown in Fig. 1, while training on only three relatively small-scale synthetic datasets, StableMTL generalizes effectively to a vast range of real-world scenarios, including unseen structures and domains significantly out-of-distribution (*e.g.*, DAVIS and Youtube-VOS), in a zero-shot fashion. Further, it outperforms existing partially labeled MTL methods on 7 tasks, across 8 benchmarks, with a remarkable  $+83.54 \Delta_m$  overall improvement.

## 2 Related works

**Multi-Task Learning (MTL).** There is a large body of literature on MTL for dense tasks, surveyed in [57], which rely on various architectural choices like task-specialized modules [51, 11, 43], dynamically adapting architectures [39, 14, 24, 1], integrating attention mechanisms for feature sharing [77, 55, 7], or use of transformer-based models [70, 68, 17]. Closer to us, the rise of large-scale pre-trained models spurred adapter-based fine-tuning methods [36, 33]. To cope with multitask objectives people uses adaptive loss weighting [29], gradient manipulations [12, 13, 72, 53], or seek Pareto-optimal solutions [44, 34]. A key aspect of MTL is how to enhance task exchange [74], which has been enforced for out-of-distribution performance [73, 52], utilizing consistency losses [38], or learning joint task spaces [46, 32]. These relation-based approaches typically rely on consistency losses or pairwise constraints, which hinder scalability and stability as task counts increases.

**MTL with partial annotation.** Early efforts addressed partially labeled shallow models [35, 76, 60], subsequent deep learning approaches like MTPSL [32], Dejavu [6], DiffusionMTL [71], and JTR [46] (see [18] for a comprehensive review) have predominantly relied on simulating missing labels within single, fully-annotated datasets. This setup not only fails to fully capture real-world complexities where annotations are naturally sparse across different data sources but also hinges on the use of real-world datasets which are expensive to annotate densely for many tasks. SemiMTL [61], which explored multi-dataset MTL, was restricted to two tasks and real-world data. Motivated by these gaps and the prohibitive cost of annotating numerous tasks on real-world data, we propose a more realistic, scalable, and challenging scenario: learning a greater number of tasks from multiple synthetic datasets, each with naturally partially overlapping sets of task annotations.

**Repurposing Latent Diffusion Models (LDMs) for dense prediction.** LDMs for image generation, known for robust representations, were first repurposed by Marigold [27, 28] for dense prediction tasks like depth estimation, demonstrating strong generalization from small synthetic datasets. Subsequent efforts extended this to other individual tasks such as geometry [19], normal estimation [69], motion [63] and also improved efficiency with enhanced sampling [22] or single-step latent regression [25, 40, 66]. In the LDM context, holistic MTL remains largely unexplored. Recently, large-scale LDM-based visual foundation models like Diception [78] and OneDiffusion [31] emerged, handling diverse tasks by training on large-scale real-world data. However, their primary focus is not on holistic MTL capabilities when restricted to synthetic-only training or small-scale, partially labeled data. Our approach is complementary, offering a method to fine-tune these models for multi-task using only small-scale, partially labeled synthetic datasets.

## 3 StableMTL

We address the problem of multi-task partially supervised learning [32] by extending it to a more realistic setting where *partial* labels are obtained from *multiple synthetic* datasets. In summary, our aim is to learn  $K$  tasks from a mixture of  $N$  synthetic datasets, where each dataset has only access to labels for fewer than  $K$  tasks.

Our method, coined StableMTL, builds on recent advances in diffusion models repurposed for dense task estimation [25] allowing us to generalize to the real domain, in a zero-shot fashion. Importantly, we frame multi-task learning as a latent regression problem thus *alleviating the need for task-specific losses and weighting*. To train our complete architecture, depicted in Fig. 2, we follow a two-stage process. In the first stage, detailed in Sec. 3.1, we fine-tune a latent diffusion model repurposed for dense prediction [25], which we adapt to multi-task learning by incorporating task tokens, a unified latent loss and a custom training scheme. For clarity, we illustrate the first stage in Fig. 8 (Appendix A.2). In the second stage, to encourage task exchange, we learn a separate task-conditioning model where interactions among tasks are modeled through a task-attention mechanism. A byproduct of our unified latent loss and our careful design choices is that StableMTL can scale to various spatial and temporal tasks without the usual need for cumbersome task balancing [18].

Our training set, detailed in Tab. 1, comprises three synthetic datasets and seven tasks. These tasks include: high-level **semantic** segmentation; two geometrical tasks, namely **normal** and **depth**; two dynamic flow-based estimations, **optical flow** (pixel displacement in screen-space) and **scene flow** (3D displacement in camera-space); and two low-level intrinsic component estimations, **shading** (grayscale irradiance for lighting) and **albedo** (diffuse reflectance for material).

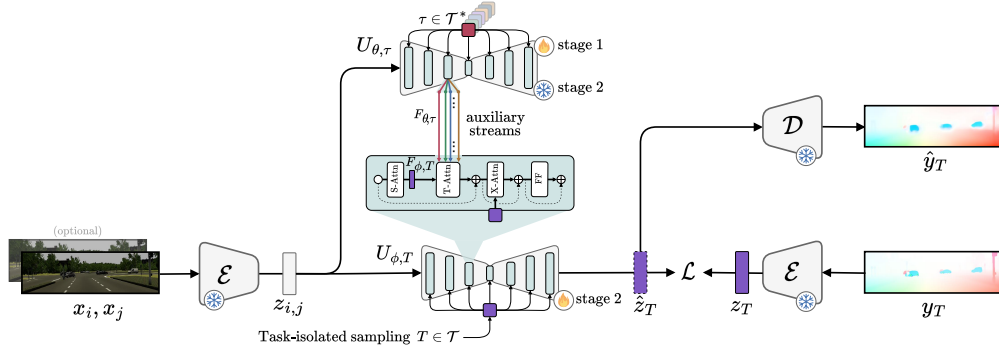


Figure 2: **Overview of StableMTL.** Our pipeline comprises two training stages. In the first stage (Sec. 3.1), we fine-tune a UNet ( $U_{\theta, \tau}$ ) to predict target annotation latents from input image latents, conditioned on multi-task tokens sampled via our training scheme to isolate task gradient (see Fig. 8 in Appendix A.2). To encourage task exchanges, the second stage (Sec. 3.2) uses a multi-stream architecture combining the frozen single-stream UNet trained during Stage 1 and a trainable *main* UNet ( $U_{\phi, T}$ ). It further benefits from a novel task attention mechanism which enriches the main UNet’s features with task-specific information from its auxiliary counterparts. Both stages are trained with a single MSE latent loss, instead of task-specific losses.

Dataset	Scene	#samples	Semantic	Normal	Depth	Optical Flow	Scene Flow	Shading	Albedo
Hypersim [49]	Indoor	39K		✓	✓			✓	✓
Virtual KITTI 2 [8]	Urban scenes	20K	✓	✓	✓	✓	✓		
Flying Things 3D [41]	Objects	20K				✓	✓		

Table 1: **Training set.** We train on an ensemble of *synthetic only* datasets, spanning over 7 tasks.

### 3.1 Single-stream architecture

Since we focus on pixel-wise tasks, we denote  $\mathbb{M} = \mathbb{R}^{H \times W}$  for brevity. Let  $x_i \in \mathbb{M}^3$  be an input image and  $y_\tau \in \mathcal{Y}_\tau$  be the corresponding annotation for a task  $\tau$  from a set of tasks  $\mathcal{T}$ . Our pipeline revolves around a latent space  $\mathcal{Z} \subset \mathbb{M}^4$  in which we perform multi-task learning. We employ the pretrained StableDiffusion [50] VAE consisting of a frozen encoder  $\mathcal{E} : \mathbb{M}^3 \rightarrow \mathcal{Z}$  and a decoder  $\mathcal{D} : \mathcal{Z} \rightarrow \mathbb{M}^3$  for the inverse operation. An image latent is computed directly as  $z_i = \mathcal{E}(x_i)$ . Considering annotations  $y_\tau$  are of different nature and encoding (e.g., **semantic** encodes discrete class indices while **depth** is continuous), tasks must first be processed by a task-specific function  $f_\tau : \mathcal{Y}_\tau \rightarrow \mathbb{M}^3$ . As a result, task latents are obtained as:  $z_\tau = \mathcal{E}(f_\tau(y_\tau))$ . A UNet model, denoted by  $U_\theta$ , parametrized by  $\theta$ , is fine-tuned to predict in a single step the task latent  $\hat{z}_\tau$  from the input latent  $z_i$ , i.e.,  $\hat{z}_\tau = U_\theta(z_i)$ . For tasks requiring multi-frame inputs – such as flow estimation tasks – we extend our pipeline to receive multiple input frames. At the decoding stage, a network  $\mathcal{D} : \mathcal{Z} \rightarrow \mathbb{M}^3$  maps latent representations back to the RGB space. Similarly, predicted maps  $\hat{y}_\tau$  require a post-processing step  $p_\tau : \mathbb{M}^3 \rightarrow \mathcal{Y}_\tau$  after being decoded, resulting in  $p_\tau(\mathcal{D}(\hat{z}_\tau))$ .

Unlike traditional multi-step diffusion methods [27] with iterative denoising, we employ a single-step, deterministic formulation which leads to faster training and inference times while maintaining generalization ability [25]. We extend such models for multi-task learning by adopting task tokens, initially introduced for dense prediction by diffusion models in  $\text{RGB} \leftrightarrow \text{X}$  [75]. Such conditioning is achieved by providing the UNet with fixed token embeddings for each task  $c_\tau$  and computing cross-attention between these embeddings and the layer activations. We detail these task tokens in Appendix A.2. The UNet is predicting the task latent as  $\hat{z}_\tau = U_\theta(z_i, c_\tau)$ , written  $U_{\theta, \tau}(z_i)$  for short. Although  $\text{RGB} \leftrightarrow \text{X}$  makes use of the same mechanism, it focuses on image decomposition while we address the broader scope of multi-task learning. Our goal is to benefit from a joint learning of such tasks, but in a multi-dataset and partially-annotated setting.

**Multi-frame adaptation.** Some tasks such as flow estimation can be solved from a monocular input [2, 3] but are better conditioned using a pair of temporal frames ( $i, j$ ). To accommodate such spatio-temporal tasks, StableMTL takes as input a channel-wise concatenated pair of latents, being

$z_{i,j} = \text{concat}(z_i, z_j)$ . The model then predicts the task output as  $\hat{z}_\tau = U_{\theta,\tau}(z_{i,j})$ . For single-frame tasks (e.g., **semantic**, **depth**) we simply set  $j = i$ , thereby concatenating  $z_i$  with itself. This simple scheme provides a basis for handling both spatial and spatio-temporal tasks in a unified framework.

**Task-gradient isolation scheme.** While we use a single unified latent loss, we also observe as in classical MTL that some tasks may exhibit larger gradient magnitudes and conflicting directions [18], resulting in task with weaker gradients being dominated by the stronger ones. To address this, we adopt a task-isolation training scheme, where at each training step, each mini-batch contains only a single task. Further, during gradient accumulation – used to simulate larger batch sizes – we accumulate gradients only from mini-batches of the same task and subsequently perform an optimizer step followed by gradient resetting, before proceeding to the next task. For each task available, we minimize the Mean Squared Error (MSE) loss in the latent space between the predicted latent  $\hat{z}_\tau$  and the ground-truth latent  $z_\tau$ :

$$\mathcal{L}(\theta) = \|\hat{z}_\tau - z_\tau\|_2^2 = \|U_{\theta,\tau}(z_{i,j}) - \mathcal{E}(f_\tau(y_\tau))\|_2^2. \quad (1)$$

### 3.2 Multi-stream architecture

Our above single-stream architecture can handle multiple tasks simultaneously with task tokens, but does not incorporate any explicit tasks exchange mechanisms. Prior works have addressed this by training N tasks jointly with an N-to-N multi-task attention mechanism, where each task attends to all others to learn task interactions [7, 37]. Such strategy, however, scales poorly with the number of tasks. Therefore, we propose a multi-stream architecture, where the main stream attends tasks, processed via the single-stream (Sec. 3.1), making use of a more scalable 1-to-N attention.

**Architecture.** Our multi-stream architecture, depicted in Fig. 2, extends the single-stream architecture described above by adding an additional UNet. This *main* trainable UNet, denoted  $U_{\phi,T}$ , is responsible of the final MTL output, conditioned on a *main* task token  $T$  (e.g., [token]). The single-stream UNet trained in Sec. 3.1, denoted  $U_{\theta,\tau}$ , is kept frozen and referred as *auxiliary* since it generates task-specific feature streams, for auxiliary tasks, beneficial for solving the main task. During inference,  $U_{\theta,\tau}$  produces auxiliary streams for all tasks  $\tau$ , other than the main task  $T$ . The main UNet  $U_{\phi,T}$  then predicts the output for  $T$ , while attending to these auxiliary features. The training of  $U_{\phi,T}$  is similar to Sec. 3.1, with its weights initialized from  $U_{\theta,\tau}$ .

**Task attention.** The UNet is comprised of stacked 2D convolutional residual blocks and transformer blocks. Each transformer block contains a spatial attention layer (S-Attn), a cross-attention layer (X-Attn), and a feed-forward network (FF). Spatial attention aggregates information from correlated 2D spatial locations, while cross-attention conditions the features on the task token. In the main UNet,  $U_{\phi,T}$ , we introduce an additional task-attention layer within each transformer block, placed immediately after the spatial (self-)attention layer. This new layer enriches the main stream features by attending to relevant task-specific features from the auxiliary streams, as depicted in Fig. 3.

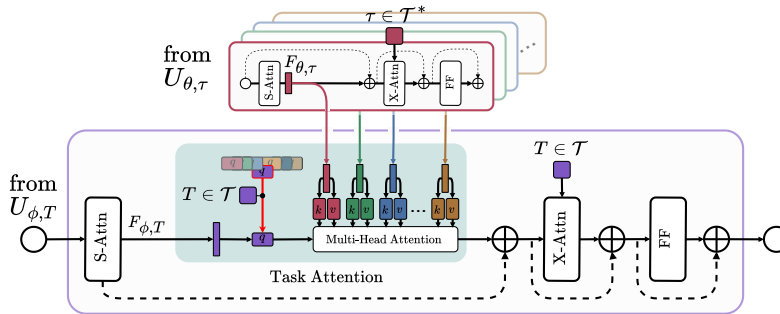


Figure 3: **Proposed task attention.** In addition to standard spatial and cross-attention mechanisms, our transformer blocks in the main UNet incorporate multi-stream information from auxiliary tasks. This is achieved by connecting the dedicated frozen single-stream UNet ( $U_{\theta,\tau}$ ) to the main UNet ( $U_{\phi,T}$ ), providing the latter with auxiliary features.  $U_{\theta,\tau}$  is kept frozen.

We define  $F_{\phi,T}$  as the feature map from the spatial attention layer in the main UNet  $U_{\phi,T}$ , conditioned on task  $T$ . Let  $\mathcal{T}^* = \mathcal{T} \setminus \{T\}$  and  $\{F_{\theta,\tau} \mid \tau \in \mathcal{T}^*\}$  be the set of corresponding feature maps from the frozen auxiliary UNet  $U_{\theta,\tau}$  (the auxiliary streams), each conditioned on an auxiliary task token  $\tau$ . The cross-attention from the main stream to the auxiliary streams is computed as  $\text{Attention}(Q, K, V) = \text{softmax}(QK^\top / \sqrt{d})V$ , where

$$Q = [q_T(F_{\phi,T})], \quad K = [k_\tau(F_{\theta,\tau}) \mid \tau \in \mathcal{T}^*], \quad V = [v_\tau(F_{\theta,\tau}) \mid \tau \in \mathcal{T}^*], \quad (2)$$

and  $d$  is the feature dimension. Each task  $t$  has its own projection layers  $(q_t, k_t, v_t)$ , enabling task-specific adaptation. The brackets  $[\cdot]$  denote concatenation along a newly introduced *task* dimension, conceptually achieved via an `unsqueeze` operation followed by concatenation.

**Attention-guided task masking.** As previously mentioned, both the main UNet  $U_{\phi,T}$  and the auxiliary UNet  $U_{\theta,\tau}$  are initialized with identical pretrained weights from our single-stream training. This shared initialization can cause the task attention mechanism to concentrate heavily (become "spiky") on a few auxiliary tasks early in training. To promote broader exploration and prevent attention saturation, we implement attention-guided task masking within each task-attention layer.

For each spatial location (*i.e.*, "image token") in every task-attention layer,  $(s_{T \rightarrow \tau})_{\tau \in \mathcal{T}^*}$  denotes the vector of attention scores from the main stream (task  $T$ ) to the auxiliary streams (tasks  $\tau \in \mathcal{T}^*$ ). These scores are computed as components of  $\text{softmax}(QK^\top / \sqrt{d})$  and represent the attention assigned by task  $T$  to auxiliary task  $\tau$ . Intuitively, tasks with higher scores should have a higher chance of being masked. We model this with the distribution  $\pi_T$  over auxiliary tasks  $\mathcal{T}^*$ :  $\pi_T(\tau) = \frac{s_{T \rightarrow \tau}}{\sum_{\tau \in \mathcal{T}^*} s_{T \rightarrow \tau}}$ .

To select a task for masking, we proceed by sampling  $m_T \sim \text{Sample}(\pi_T)$  which results in per-task masks:  $M(t) = \mathbb{1}[t \neq m_T]$ , where  $\mathbb{1}$  is the indicator function. This mask is then applied when computing the attention score  $\{M(\tau) * s_{T \rightarrow \tau} \mid \tau \in \mathcal{T}^*\}$ . To push exploration, we stochastically apply the masking procedure with probability  $\rho$ . We later ablate the impact of  $\rho$  and alternative sampling strategies. This encourages diverse task combinations and prevents over-reliance on dominant tasks.

## 4 Experiments

**Datasets.** As listed in Tab. 1, we train our model for seven tasks using three synthetic datasets: Hypersim [49], VKITTI 2 [8], and FlyingThings3D [41]. At each training step, we first uniformly sample a task. If the selected task is labeled in multiple datasets, we sample from a specific dataset according to the following probabilities: for **depth** and **normal**, we use the sampling as Marigold [27]; for **optical flow** and **scene flow**, we sample FlyingThings3D and VKITTI 2 equally.

For evaluation, we leverage real image datasets. **Normal** is evaluated on DIODE [58]; **depth** on KITTI [20] and DIODE [58]; **semantic** on Cityscapes [15] with the class mapping from [37]; **optical flow** and **scene flow** on KITTI flow [42]; lastly we use MIDIntrinsics [45, 9] for **shading** and **albedo**. Additional real-world datasets are leveraged for qualitative results. Details are in Appendix A.4.

**Baselines.** We highlight that most MTL methods are designed to be trained on fully annotated datasets, thus not directly comparable. We therefore compare to [71, 46], which also handle partial annotations. Since both DiffusionMTL [71] and JTR [46] are trained with **semantic**, **normal**, and **depth** at most, we report these numbers by training on our ensemble of datasets using the baselines losses and loss weights. For a more direct comparison with our method, we also put significant efforts to adapt baselines to our full multi-dataset and full task set  $\mathcal{T}$  setting, including support of temporal tasks which required modification of the architectures. Adaptations are reported as DiffusionMTL\* and JTR\*. Furthermore, since our single-stream architecture (Sec. 3.1) is also capable of performing multitask, we include its results as StableMTL- $\mathcal{S}$ .

**Metrics.** We rely on mean intersection over union (mIoU) for **semantic**; absolute relative error (AbsRel) for **depth**; mean angular error in degrees (mAE) for **normal**; average endpoint error for **optical flow** (EPE-2D) and **scene flow** (EPE-3D); and root mean squared error (RMSE) for **shading** and **albedo**. For tasks with unbounded quantities, we first perform a per-channel least squares fitting against the ground truth [27, 9]. The delta metric ( $\Delta_m$ ) is used to quantify multi-task performance [57]. It measures the average relative performance over all tasks for a given model compared to its single-task counterparts. For **depth**, the  $\Delta_m$  is averaged over two datasets.

**Implementation.** We provide details on how each task is encoded into the latent space in Appendix A.1. Our architecture follows Lotus-D [25] (discriminative variant) without its detail preserver.

Method	Semantic	Normal	Depth		Opt. Flow	Sc. Flow	Shading	Albedo	MTL Perf.
	mIoU % $\uparrow$	mAE $\downarrow$	AbsRel % $\downarrow$	AbsRel % $\downarrow$	EPE-2D px $\downarrow$	EPE-3D m $\downarrow$	RMSE $\downarrow$	RMSE $\downarrow$	$\Delta_m$ % $\uparrow$
	Cityscapes	DIODE	KITTI	DIODE	KITTI	KITTI	MID	MID	Average
Single-task baseline	48.17	22.27	14.21	32.56	10.36	0.2735	0.2145	0.2551	0.00
JTR [46]	45.75	40.23	26.39	66.39	n/a	n/a	n/a	n/a	-
JTR* [46]	20.46	50.91	39.27	73.14	34.92	0.5176	0.3030	0.3565	-106.87
DiffusionMTL [71]	30.09	35.64	21.10	45.19	n/a	n/a	n/a	n/a	-
DiffusionMTL* [71]	45.92	44.56	24.83	58.17	36.60	0.3502	0.3004	0.3660	-78.76
StableMTL-S	52.57	23.94	15.64	33.36	12.76	0.2618	0.2310	0.2077	-1.57
StableMTL	55.79	23.27	14.98	33.03	10.76	0.2313	0.2346	0.2016	+4.78

Table 2: **Multi-task performance.** StableMTL significantly expands task coverage, addressing over twice the tasks of original baselines, while consistently outperforming them on individual tasks and multi-task metric. **best** and **second-best** are highlighted. \* baselines adapted to full setting

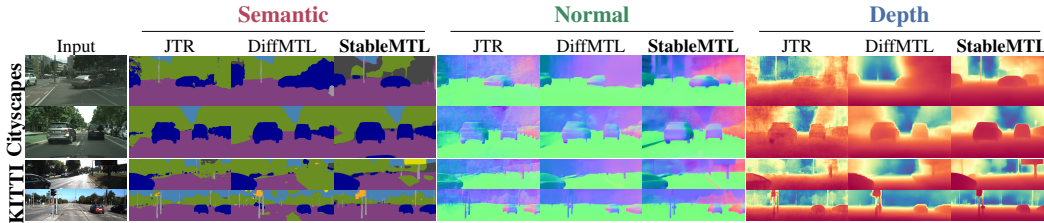


Figure 4: **Qualitative comparison.** We compare against original baseline versions as these are better performing (*cf.* Tab. 2) than the adapted full setting variants on the three tasks displayed. StableMTL demonstrates superior qualitative results.

To accommodate two-frame inputs, we triple the number of input channels in the first convolution of  $U_{\phi,T}$ . We initialize the expanded weights and dividing them by three as in [27]. We insert our task-attention layers at each of the 16 transformer blocks of  $U_{\phi,T}$ . We employ multi-head attention [59] to foster learning diversity. Our optimal model uses four attention heads, discussed in Sec. 4.2.

#### 4.1 Main results

Tab. 2 compares our method with 4 baselines on 8 benchmarks across 7 tasks. When comparing StableMTL with the best baseline in each task, we observe a significant boost across all tasks, exemplified by improvements such as +9.87 mIoU (**semantic**), a -12.37 mAE (**normal**), and a -0.1189 EPE-3D (**scene flow**). Notably, our method improves the overall multi-task performance by +83.54  $\Delta_m$ . Furthermore, our single-stream version, StableMTL-S, underperforms single-task baseline with a -1.57  $\Delta_m$  in overall MTL performance, our complete model, StableMTL, improves the overall performance by +4.78  $\Delta_m$ , showing the benefits of our multi-stream architecture and inter-task attention. We highlight that because DiffusionMTL and JTR use task-specific losses, they are difficult to scale architecturally and their training is unstable with a large number of tasks. Note how **normal** and **depth** degrade in the full setting (e.g., comparing JTR\* and JTR). We further assess qualitative results in Fig. 4, demonstrating that StableMTL consistently outperforms the baselines. Additional results on real-world datasets [15, 42, 56, 64, 23, 65, 67, 48] are in Figs. 1 and 11, showing our method generalizes, in a zero-shot fashion, to diverse out-of-distribution domains.

#### 4.2 Discussion

**Impact of training datasets.** Tab. 3 shows that removing individual datasets degrades performance, depending on domain similarity and annotation quality. For example, removing VKITTI 2 for flow tasks (row #2) leads to bigger performance degradation, especially on **sc. flow** and **opt. flow**, compared to removing FlyingThings3D (row #3), which shows VKITTI 2 better aligns with our evaluation domain. Removing Hypersim for geometrical tasks (row #5) drastically impacts **depth** and **normal**, especially on the DIODE dataset, which may result from its higher annotation quality and domain match. Interestingly, KITTI **depth** exhibits similar drops regardless of the dataset removed,

	Seg. & Sha. & Alb.	Opt.Flow & Sc.Flow		Normal & Depth		Semantic	Normal	Depth		Opt. Flow	Sc. Flow	Shading	Albedo	MTL Perf.
	Hypersim & Virtual KITTI 2	Virtual KITTI 2	Flying Things 3D	Virtual KITTI 2	Hypersim	mIoU % $\uparrow$	mAE $\downarrow$	AbsRel % $\downarrow$	AbsRel % $\downarrow$	EPE-2D px $\downarrow$	EPE-3D m $\downarrow$	RMSE $\downarrow$	RMSE $\downarrow$	$\Delta_m$ % $\uparrow$
						Cityscapes	DIODE	KITTI	DIODE	KITTI	KITTI	MID	MID	Avg
#1	✓	✓	✓	✓	✓	55.08	23.36	14.03	32.97	11.22	0.2297	0.2350	0.2061	+4.14
#2	✓	-	✓	✓	✓	53.47	23.69	13.74	33.54	24.15	0.4126	0.2367	0.2103	-24.30
#3	✓	-	-	✓	✓	55.28	22.29	14.82	33.21	13.60	0.2541	0.2383	0.2012	+0.01
#4	✓	✓	✓	-	✓	44.55	23.79	17.98	34.13	11.99	0.2456	0.2236	0.2110	-3.10
#5	✓	✓	✓	-	-	50.12	52.65	18.26	45.27	12.40	0.2484	0.2279	0.2107	-23.46

Table 3: **Ablation study of training datasets.** Removing task supervision from any dataset degrades performance on the corresponding tasks (*cf.* text for details). We highlight **best** and **second-best**.

Method	Semantic	Normal	Depth		Opt. Flow	Scene Flow	Shading	Albedo	MTL Perf.
	mIoU % $\uparrow$	mAE $\downarrow$	AbsRel % $\downarrow$	AbsRel % $\downarrow$	EPE-2D px $\downarrow$	EPE-3D m $\downarrow$	RMSE $\downarrow$	RMSE $\downarrow$	$\Delta_m$ % $\uparrow$
	Cityscapes	DIODE	KITTI	DIODE	KITTI	KITTI	MID	MID	Avg
StableMTL( $\rho=0$ )	54.90	22.88	14.90	32.57	11.45	0.2400	0.2351	0.2023	+3.41
w/o separate ( $q_t, k_t, v_t$ )	48.38	24.15	16.17	33.24	11.06	0.2327	0.2295	0.2066	+0.85
w/o single-stream init.	44.69	23.35	15.60	33.21	12.17	0.2647	0.2325	0.2110	-3.11
w/o multi-stream	52.57	23.94	15.64	33.36	12.76	0.2618	0.2310	0.2077	-1.57

Table 4: **Multi-stream ablation.** Each design choice contributes to the best performance.

suggesting that VKITTI 2’s domain proximity offsets its lower annotation quality, while Hypersim’s quality alone cannot overcome the larger domain gap.

**Multi-stream ablation.** In Tab. 4, we conduct an ablation study on various design choices of StableMTL. Removing separate projection layer per task *i.e.*, "w/o separate ( $q_t, k_t, v_t$ )" improves performance on certain tasks like **optical flow**, **scene flow**, and **shading**, but degrades others and leads to an overall multi-task drop of 2.56 in  $\Delta_m$ . This might be attributed to the highly similar attention patterns across tasks illustrated in Fig. 10, which limits the learned inter-task interaction. Initializing  $U_\phi$  with Stable Diffusion weights instead of  $U_\theta$  *i.e.*, "w/o single-stream init.", significantly degrades performance by 6.52 in  $\Delta_m$ . We also report using only single-stream *i.e.*, "w/o multi-stream" also degrading performance on all tasks (drop of 4.98 in  $\Delta_m$ ), since the single stream does not benefit from cross-task exchanges. Additionally, we ablate our multi-frame adaptation on the single-stream only for single-input tasks, with ours being  $z_{i,j} = \text{concat}(z_i, z_j)$ , compared to  $z_{i,j} = \text{avg}(z_i, z_j)$ , and  $z_{i,j} = \text{concat}(z_i, \emptyset)$ ; they perform  $-1.57$ ,  $-4.11$ , and  $-2.72$  in  $\Delta_m$ , respectively.

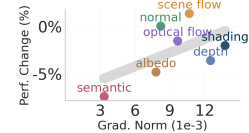
**Benefit of task-gradient isolation.** Figure 5a demonstrates the efficacy of our isolation scheme, which improves overall performance by 2.54  $\Delta_m$ . In particular, it drastically improves **semantic** and **albedo**, which have lower gradient norm as seen in Fig. 5b. The latter further reveals an inverse relationship between gradient norms and the performance drop when removing our isolation scheme. Without this scheme, tasks with smaller gradient exhibit large performance drops.

**Effects of task attention heads.** Varying task attention to use 1/2/4/8 heads leads to an overall performance of  $+2.45/+4.14/+4.78/+4.41$  in  $\Delta_m$ , respectively. As is evident, although more heads promote greater attention, a plateau is quickly reached, likely due to the reduced capacity of each head. Notably, all outperform the single-stream StableMTL-S, which achieved  $-1.57$   $\Delta_m$ .

**Impact of training tasks.** Figure 6 shows performance on **semantic** and **normal** when training on different set tasks w.r.t. single-task performance. Adding new tasks to the pipeline affects single-task

Method	Semantic	Normal	Depth		Opt. Flow	Scene Flow	Shading	Albedo	MTL Perf.
	mIoU % $\uparrow$	mAE $\downarrow$	AbsRel % $\downarrow$	AbsRel % $\downarrow$	EPE-2D px $\downarrow$	EPE-3D m $\downarrow$	RMSE $\downarrow$	RMSE $\downarrow$	$\Delta_m$ % $\uparrow$
	Cityscapes	DIODE	KITTI	DIODE	KITTI	KITTI	MID	MID	Avg
StableMTL-S	52.57	23.94	15.64	33.36	12.76	0.2618	0.2310	0.2077	-1.57
w/o Task-gradient isolation	48.68	23.93	15.52	34.82	12.96	0.2583	0.2379	0.2178	-4.11

(a) Ablation of task-grad. isolation training scheme.



(b) Observed correlation

Figure 5: **Task-gradient isolation strategy.** In (a), we report the performance w/ and w/o our isolation strategy, showing that it drastically benefits some tasks (*e.g.*, **semantic**) and improves the overall  $\Delta_m$  metric. (b) shows that when removing gradient isolation, tasks with smaller gradient magnitudes are overwhelmed by those with larger ones, leading to a significant performance drop.

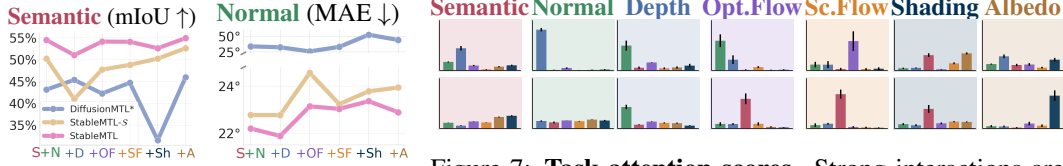


Figure 6: **Tasks ablation.** Separate trainings with increasing task counts.

Figure 7: **Task attention scores.** Strong interactions are observed not only among tasks with known mutual benefits but also one-way interactions, as detailed in the text.

Strategy	Prob. ( $\rho$ )	Semantic	Normal	Depth		Opt. Flow	Scene Flow	Shading	Albedo	MTL Perf.
		mIoU % $\uparrow$ Cityscapes	mAE % $\downarrow$ DIODE	AbsRel % $\downarrow$ KITTI	AbsRel % $\downarrow$ DIODE	EPE-2D px $\downarrow$ KITTI	EPE-3D m $\downarrow$ KITTI	RMSE $\downarrow$ MID	RMSE $\downarrow$ MID	$\Delta_m$ % $\uparrow$ Avg
Sample( $\pi_T$ )	0.0	54.90	22.88	14.90	32.57	11.45	0.2400	0.2351	0.2023	+3.41
	0.2	54.86	23.49	14.71	32.61	11.00	0.2378	0.2349	0.2047	+3.70
	<b>0.4</b>	55.08	23.36	14.03	32.97	11.22	0.2297	0.2350	0.2061	+4.14
	0.6	53.97	23.26	15.22	32.94	10.90	0.2284	0.2348	0.2029	+4.00
Sample $_k$ ( $\pi_T$ )	0.8	52.95	23.02	14.73	32.89	11.21	0.2386	0.2349	0.2093	+2.72
	0.4	54.65	23.82	15.02	33.15	10.96	0.2311	0.2338	0.2064	+3.50
	argmax	54.45	23.09	14.98	32.87	11.22	0.2299	0.2339	0.2071	+3.65
	$\mathcal{U}(T)$	54.77	22.69	15.02	32.70	11.32	0.2398	0.2313	0.2057	+3.60

Table 5: **Ablation of attention masking.** Masking heads depending on their attention score using our distribution Sample( $\pi_T$ ) boosts performance by encouraging exploration. On the contrary, other methods, detailed in the text, perform worse. **Best** and **Second-best** are highlighted.

performance, which is a clear issue for StableMTL-S but somehow is mitigated by the multi-stream architecture of StableMTL thanks to its task-attention mechanism leveraging inter-task information.

**Visualization of task attentions.** Figure 7 shows the task attention scores from main stream tasks (columns) to auxiliary stream tasks (represented by colored bars) at selected layers: here, layer 12 and 15 – more layers shown in Appendix A.5). The observed patterns reveal strong mutually interactions like **normal/depth**, **optical flow/scene flow**, and **shading/albedo**, but also that some tasks are one-way beneficiaries of others such as **optical flow** using **semantic** and **semantic** using **shading**. Notably, **shading** and **albedo**, capturing lighting and material properties, respectively, can assist other tasks. These interactions support the findings of a prior work [74].

**Effect of task attention masking.** We ablate the task attention masking in Tab. 5. Masking a single task proportional to its attention weight (Sample( $\pi_T$ )) improves performance as the masking probability  $\rho$  increases to an optimum (*i.e.*,  $\rho=4$ ), as this fosters exploration of diverse task combinations. However, higher  $\rho$  values produces excessive exploration, lowering performance. Consequently, masking a random number of  $k$  tasks at once (Sample $_k$ ( $\pi_T$ )) is less effective. Other approaches are also suboptimal: dropping the highest-attention task (argmax) prevents exploitation of the strongest signal, while randomly dropping tasks ( $\mathcal{U}(T)$ ) offers a weaker exploration incentive.

**Limitations.** We observe that despite enhancing multi-task capabilities, StableMTL performance on some individual tasks lags behind single-task models. Furthermore, adding some new tasks (*e.g.*, shading) affects the individual performances on other tasks as evidenced in Fig. 6, showing that cross-task interaction is far from optimal yet. In terms of inference, multi-task prediction is currently sequential. We believe this is a constraint that future work could address with models enabling simultaneous multi-output prediction via improved multi-token conditioning. Additionally, the uniform task sampling strategy could be refined through adaptive approaches.

## 5 Conclusion

This work extends the task of partially supervised MTL to a more practical setting where the model is trained on multiple synthetic datasets with partial labels. To bridge the synthetic-to-real gap, we adapt a single-step latent diffusion model with multi-task encoding and task-gradient isolation. While this model is capable of multi-tasking, it suffers from degraded overall performance. To overcome this limitation, we introduce a multi-stream architecture with task attention, allowing the model to leverage inter-task relationships and improve multi-task performance. Our approach not only scales to more tasks, it also achieves significant results on unseen data.

## References

- [1] Aich, A., Schuler, S., Roy-Chowdhury, A.K., Chandraker, M., Suh, Y.: Efficient controllable multi-task architectures. In: ICCV (2023)
- [2] Aleotti, F., Poggi, M., Mattoccia, S.: Learning optical flow from still images. In: CVPR (2021)
- [3] Argaw, D.M., Kim, J., Rameau, F., Cho, J.W., Kweon, I.S.: Optical flow estimation from a single motion-blurred image. In: AAAI (2021)
- [4] Bae, G., Davison, A.J.: Rethinking inductive biases for surface normal estimation. In: CVPR (2024)
- [5] Baker, S., Roth, S., Scharstein, D., Black, M.J., Lewis, J., Szeliski, R.: A database and evaluation methodology for optical flow. In: ICCV (2007)
- [6] Borse, S., Das, D., Park, H., Cai, H., Garrepalli, R., Porikli, F.: Dejavu: Conditional regenerative learning to enhance dense prediction. In: CVPR (2023)
- [7] Brüggemann, D., Kanakis, M., Obukhov, A., Georgoulis, S., Van Gool, L.: Exploring relational context for multi-task dense prediction. In: ICCV (2021)
- [8] Cabon, Y., Murray, N., Humenberger, M.: Virtual kitti 2. In: arXiv (2020)
- [9] Careaga, C., Aksoy, Y.: Intrinsic image decomposition via ordinal shading. ACM TOG (2023)
- [10] Careaga, C., Aksoy, Y.: Colorful diffuse intrinsic image decomposition in the wild. ACM TOG (2024)
- [11] Chen, T., Chen, X., Du, X., Rashwan, A., Yang, F., Chen, H., Wang, Z., Li, Y.: AdaMV-MoE: Adaptive multi-task vision mixture-of-experts. In: ICCV (2023)
- [12] Chen, Z., Badrinarayanan, V., Lee, C.Y., Rabinovich, A.: Gradnorm: Gradient normalization for adaptive loss balancing in deep multitask networks. In: ICML (2018)
- [13] Chen, Z., Ngiam, J., Huang, Y., Luong, T., Kretzschmar, H., Chai, Y., Anguelov, D.: Just pick a sign: Optimizing deep multitask models with gradient sign dropout. In: NeurIPS (2020)
- [14] Choi, W., Im, S.: Dynamic neural network for multi-task learning searching across diverse network topologies. In: CVPR (2023)
- [15] Cordts, M., Omran, M., Ramos, S., Rehfeld, T., Enzweiler, M., Benenson, R., Franke, U., Roth, S., Schiele, B.: The cityscapes dataset for semantic urban scene understanding. In: CVPR (2016)
- [16] Eigen, D., Puhrsch, C., Fergus, R.: Depth map prediction from a single image using a multi-scale deep network. In: NeurIPS (2014)
- [17] Fan, Z., Sarkar, R., Jiang, Z., Chen, T., Zou, K., Cheng, Y., Hao, C., Wang, Z., et al.: M<sup>3</sup>VIT: Mixture-of-experts vision transformer for efficient multi-task learning with model-accelerator co-design. In: NeurIPS (2022)
- [18] Fontana, M., Spratling, M., Shi, M.: When multitask learning meets partial supervision: A computer vision review. Proceedings of the IEEE (2024)
- [19] Fu, X., Yin, W., Hu, M., Wang, K., Ma, Y., Tan, P., Shen, S., Lin, D., Long, X.: Geowizard: Unleashing the diffusion priors for 3d geometry estimation from a single image. In: ECCV (2024)
- [20] Geiger, A., Lenz, P., Urtasun, R.: Are we ready for autonomous driving? the kitti vision benchmark suite. In: CVPR (2012)
- [21] Ghiasi, G., Zoph, B., Cubuk, E.D., Le, Q.V., Lin, T.Y.: Multi-task self-training for learning general representations. In: ICCV (2021)

- [22] Gui, M., Schusterbauer, J., Prestel, U., Ma, P., Kotovenko, D., Grebenkova, O., Baumann, S.A., Hu, V.T., Ommer, B.: DepthFM: Fast monocular depth estimation with flow matching. In: AAAI (2025)
- [23] Guizilini, V., Ambrus, R., Pillai, S., Raventos, A., Gaidon, A.: 3d packing for self-supervised monocular depth estimation. In: CVPR (2020)
- [24] Guo, P., Lee, C.Y., Ulbricht, D.: Learning to branch for multi-task learning. In: ICML (2020)
- [25] He, J., Li, H., Yin, W., Liang, Y., Li, L., Zhou, K., Liu, H., Liu, B., Chen, Y.C.: Lotus: Diffusion-based visual foundation model for high-quality dense prediction. In: ICLR (2025)
- [26] He, K., Zhang, X., Ren, S., Sun, J.: Deep residual learning for image recognition. In: CVPR (2016)
- [27] Ke, B., Obukhov, A., Huang, S., Metzger, N., Daudt, R.C., Schindler, K.: Repurposing diffusion-based image generators for monocular depth estimation. In: CVPR (2024)
- [28] Ke, B., Qu, K., Wang, T., Metzger, N., Huang, S., Li, B., Obukhov, A., Schindler, K.: Marigold: Affordable adaptation of diffusion-based image generators for image analysis. T-PAMI (2025)
- [29] Kendall, A., Gal, Y., Cipolla, R.: Multi-task learning using uncertainty to weigh losses for scene geometry and semantics. In: CVPR (2018)
- [30] Kingma, D.P., Ba, J.: Adam: A method for stochastic optimization. In: ICLR (2015)
- [31] Le, D.H., Pham, T., Lee, S., Clark, C., Kembhavi, A., Mandt, S., Krishna, R., Lu, J.: One diffusion to generate them all. In: CVPR (2025)
- [32] Li, W.H., Liu, X., Bilen, H.: Learning multiple dense prediction tasks from partially annotated data. In: CVPR (2022)
- [33] Liang, X., Wu, Y., Han, J., Xu, H., Xu, C., Liang, X.: Effective adaptation in multi-task co-training for unified autonomous driving. In: NeurIPS (2022)
- [34] Lin, X., Zhen, H.L., Li, Z., Zhang, Q.F., Kwong, S.: Pareto multi-task learning. In: NeurIPS (2019)
- [35] Liu, Q., Liao, X., Carin, L.: Semi-supervised multitask learning. In: NeurIPS (2007)
- [36] Liu, Y.C., Ma, C.Y., Tian, J., He, Z., Kira, Z.: Polyhistor: Parameter-efficient multi-task adaptation for dense vision tasks. In: NeurIPS (2022)
- [37] Lopes, I., Vu, T.H., de Charette, R.: DenseMTL: Cross-task attention mechanism for dense multi-task learning. In: WACV (2023)
- [38] Lu, Y., Pirk, S., Dlabal, J., Brohan, A., Pasad, A., Chen, Z., Casser, V., Angelova, A., Gordon, A.: Taskology: Utilizing task relations at scale. In: CVPR (2021)
- [39] Lu, Y., Kumar, A., Zhai, S., Cheng, Y., Javidi, T., Feris, R.: Fully-adaptive feature sharing in multi-task networks with applications in person attribute classification. In: CVPR (2017)
- [40] Martin Garcia, G., Abou Zeid, K., Schmidt, C., de Geus, D., Hermans, A., Leibe, B.: Fine-tuning image-conditional diffusion models is easier than you think. In: WACV (2025)
- [41] Mayer, N., Ilg, E., Häusser, P., Fischer, P., Cremers, D., Dosovitskiy, A., Brox, T.: A large dataset to train convolutional networks for disparity, optical flow, and scene flow estimation. In: CVPR (2016)
- [42] Menze, M., Geiger, A.: Object scene flow for autonomous vehicles. In: CVPR (2015)
- [43] Misra, I., Shrivastava, A., Gupta, A., Hebert, M.: Cross-stitch networks for multi-task learning. In: CVPR (2016)
- [44] Momma, M., Dong, C., Liu, J.: A multi-objective/multi-task learning framework induced by pareto stationarity. In: ICML (2022)

- [45] Murmann, L., Gharbi, M., Aittala, M., Durand, F.: A multi-illumination dataset of indoor object appearance. In: ICCV (2019)
- [46] Nishi, K., Kim, J., Li, W., Pfister, H.: Joint-task regularization for partially labeled multi-task learning. In: CVPR (2024)
- [47] Ouali, Y., Hudelot, C., Tami, M.: Semi-supervised semantic segmentation with cross-consistency training. In: CVPR (2020)
- [48] Perazzi, F., Pont-Tuset, J., McWilliams, B., Gool, L.V., Gross, M., Sorkine-Hornung, A.: A benchmark dataset and evaluation methodology for video object segmentation. In: CVPR (2016)
- [49] Roberts, M., Ramapuram, J., Ranjan, A., Kumar, A., Bautista, M.A., Paczan, N., Webb, R., Susskind, J.M.: Hypersim: A photorealistic synthetic dataset for holistic indoor scene understanding. In: ICCV (2021)
- [50] Rombach, R., Blattmann, A., Lorenz, D., Esser, P., Ommer, B.: High-resolution image synthesis with latent diffusion models. In: CVPR (2022)
- [51] Ruder, S., Bingel, J., Augenstein, I., Søgaard, A.: Latent multi-task architecture learning. In: AAAI (2019)
- [52] Saha, S., Obukhov, A., Paudel, D.P., Kanakis, M., Chen, Y., Georgoulis, S., Van Gool, L.: Learning to relate depth and semantics for unsupervised domain adaptation. In: CVPR (2021)
- [53] Senushkin, D., Patakin, N., Kuznetsov, A., Konushin, A.: Independent component alignment for multi-task learning. In: CVPR (2023)
- [54] Standley, T., Zamir, A.R., Chen, D., Guibas, L., Malik, J., Savarese, S.: Which tasks should be learned together in multi-task learning? In: ICML (2020)
- [55] Sun, K., Xiao, B., Liu, D., Wang, J.: Deep high-resolution representation learning for human pose estimation. In: CVPR (2019)
- [56] Sun, P., Kretschmar, H., Dotiwalla, X., Chouard, A., Patnaik, V., Tsui, P., Guo, J., Zhou, Y., Chai, Y., Caine, B., Vasudevan, V., Han, W., Ngiam, J., Zhao, H., Timofeev, A., Ettinger, S., Krivokon, M., Gao, A., Joshi, A., Zhang, Y., Shlens, J., Chen, Z., Anguelov, D.: Scalability in perception for autonomous driving: Waymo open dataset. In: CVPR (2020)
- [57] Vandenhende, S., Georgoulis, S., Van Gansbeke, W., Proesmans, M., Dai, D., Van Gool, L.: Multi-task learning for dense prediction tasks: A survey. T-PAMI (2022)
- [58] Vasiljevic, I., Kolkin, N., Zhang, S., Luo, R., Wang, H., Dai, F.Z., Daniele, A.F., Mostajabi, M., Basart, S., Walter, M.R., Shakhnarovich, G.: DIODE: A Dense Indoor and Outdoor DEpth Dataset. CoRR (2019)
- [59] Vaswani, A., Shazeer, N., Parmar, N., Uszkoreit, J., Jones, L., Gomez, A.N., Kaiser, Ł., Polosukhin, I.: Attention is all you need. In: NeurIPS (2017)
- [60] Wang, F., Wang, X., Li, T.: Semi-supervised multi-task learning with task regularizations. In: ICDM (2009)
- [61] Wang, Y., Tsai, Y.H., Hung, W.C., Ding, W., Liu, S., Yang, M.H.: Semi-supervised multi-task learning for semantics and depth. In: WACV (2022)
- [62] Wang, Z., Bovik, A., Sheikh, H., Simoncelli, E.: Image quality assessment: from error visibility to structural similarity. TIP (2004)
- [63] Wang, Z., Li, H., Sui, L., Zhou, T., Jiang, H., Nie, L., Liu, S.: StableMotion: Repurposing diffusion-based image priors for motion estimation. In: arXiv (2025)
- [64] Wilson, B., Qi, W., Agarwal, T., Lambert, J., Singh, J., Khandelwal, S., Pan, B., Kumar, R., Hartnett, A., Pontes, J.K., Ramanan, D., Carr, P., Hays, J.: Argoverse 2: Next generation datasets for self-driving perception and forecasting. In: NeurIPS (2021)

- [65] Xiao, P., Shao, Z., Hao, S., Zhang, Z., Chai, X., Jiao, J., Li, Z., Wu, J., Sun, K., Jiang, K., Wang, Y., Yang, D.: PandaSet: Advanced sensor suite dataset for autonomous driving. In: ITSC (2021)
- [66] Xu, G., Ge, Y., Liu, M., Fan, C., Xie, K., Zhao, Z., Chen, H., Shen, C.: What matters when repurposing diffusion models for general dense perception tasks? In: ICLR (2025)
- [67] Xu, N., Yang, L., Fan, Y., Yang, J., Yue, D., Liang, Y., Price, B., Cohen, S., Huang, T.: Youtube-vos: Sequence-to-sequence video object segmentation. In: ECCV (2018)
- [68] Xu, X., Zhao, H., Vineet, V., Lim, S.N., Torralba, A.: Mtformer: Multi-task learning via transformer and cross-task reasoning. In: ECCV (2022)
- [69] Ye, C., Qiu, L., Gu, X., Zuo, Q., Wu, Y., Dong, Z., Bo, L., Xiu, Y., Han, X.: StableNormal: Reducing diffusion variance for stable and sharp normal. ACM TOG (2024)
- [70] Ye, H., Xu, D.: Inverted pyramid multi-task transformer for dense scene understanding. In: ECCV (2022)
- [71] Ye, H., Xu, D.: DiffusionMTL: Learning multi-task denoising diffusion model from partially annotated data. In: CVPR (2024)
- [72] Yu, T., Kumar, S., Gupta, A., Levine, S., Hausman, K., Finn, C.: Gradient surgery for multi-task learning. In: NeurIPS (2020)
- [73] Zamir, A.R., Sax, A., Cheerla, N., Suri, R., Cao, Z., Malik, J., Guibas, L.J.: Robust learning through cross-task consistency. In: CVPR (2020)
- [74] Zamir, A.R., Sax, A., Shen, W.B., Guibas, L., Malik, J., Savarese, S.: Taskonomy: Disentangling task transfer learning. In: CVPR (2018)
- [75] Zeng, Z., Deschaintre, V., Georgiev, I., Hold-Geoffroy, Y., Hu, Y., Luan, F., Yan, L.Q., Hašan, M.: RGB $\leftrightarrow$ X: Image decomposition and synthesis using material- and lighting-aware diffusion models. In: SIGGRAPH (2024)
- [76] Zhang, Y., Yeung, D.Y.: Semi-supervised multi-task regression. In: Buntine, W., Grobelnik, M., Mladenić, D., Shawe-Taylor, J. (eds.) ECML PKDD (2009)
- [77] Zhang, Z., Cui, Z., Xu, C., Jie, Z., Li, X., Yang, J.: Joint task-recursive learning for semantic segmentation and depth estimation. In: ECCV (2018)
- [78] Zhao, C., Liu, M., Zheng, H., Zhu, M., Zhao, Z., Chen, H., He, T., Shen, C.: DICEPTION: A generalist diffusion model for visual perceptual tasks. In: arXiv (2025)

**Acknowledgments.** This work was funded by the French Agence Nationale de la Recherche (ANR) with project SIGHT (ANR-20-CE23-0016) and performed with HPC resources from GENCI-IDRIS (Grants AD011014102R2, AD011014102R1, AD011014389R1, and AD011012808R3). The authors are also grateful for the resources provided by the CLEPS infrastructure from Inria Paris.

**Broader impact and ethics.** Training models for joint multi-task prediction with partially labeled synthetic data substantially lowers annotation costs, benefiting numerous applications and advancing research through its comprehensive outputs. Despite these benefits, prediction errors raise ethical concerns, particularly in high-stakes areas like autonomous driving where failures can be fatal, mandating robust safety measures and redundancy. Multi-task learning’s nature, however, might provide resilience by allowing tasks to offset each other’s errors.

## A Appendix

### A.1 Task encoding

For unbounded quantities – **depth**, **optical flow**, and **scene flow** – we adopt affine-invariant representations as in [27]. Specifically, we apply independent linear scaling by mapping values from  $[a, b]$  to  $[-1, +1]$ . Where  $(a, b)$  are the 2nd/98th percentiles for **depth** and min/max values for **optical flow** and **scene flow**. For categorical tasks such as **semantic** segmentation, the annotations are discrete,  $y_{\text{seg}} \in \llbracket 1, C \rrbracket^{H \times W}$ , for  $C$  classes in total. We define a mapping  $f_{\text{seg}} : \llbracket 1, C \rrbracket \rightarrow [-1, +1]^3$  assigning a unique RGB vector to each class. Following [10], we tone-map **albedo** and **shading** with a scalar scale, then clamp and remap the values to  $[-1, +1]$ . After appropriate scaling, we standardize all shapes to match  $\mathbb{M}^3$  by repeating channels. For **depth** and **shading** (both in  $\mathbb{M}$ ), the grayscale maps are repeated three times. For **optical flow** ( $y_{\text{o-flow}} \in \mathbb{M}^2$ ), we choose to repeat the horizontal flow once. Finally **scene flow**, **normal**, and **albedo** already belong to  $\mathbb{M}^3$ .

As a post-processing step for **semantic** segmentation, we obtain final prediction  $\hat{y}_{\text{seg}}$  by first decoding the predicted latent with  $y'_{\text{seg}} = \mathcal{D}(\hat{z}_{\text{seg}})$ , then applying nearest neighbors search in the RGB space for each pixel  $(i, j)$ :  $\hat{y}_{\text{seg}}(i, j) = \arg \min_{c \in \llbracket 1, C \rrbracket} \|\hat{y}'_{\text{seg}}(i, j) - f_{\text{seg}}(c)\|_2$ . For **optical flow**, the prediction consists of the first two channels of the decoded latent. For **depth** and **shading**, we utilize the average of the three decoded channels. Other tasks do not require any post-processing.

### A.2 Single stream architecture

For clarity, our single-stream architecture (*cf.* Sec. 3.1) is depicted in Fig. 8. We fine-tune the UNet ( $U_{\theta, \tau}$ ) to predict annotation latents from input image latents. This prediction is conditioned on task tokens, which are sampled using our custom training scheme to isolate task gradients.

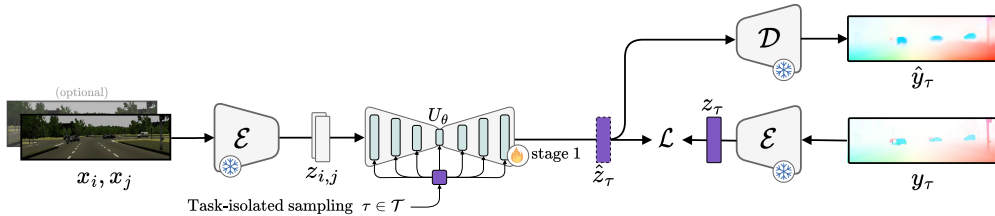


Figure 8: **Single-stream architecture.** During stage 1 (Sec. 3.1), we fine-tune a UNet ( $U_{\theta, \tau}$ ) to perform latent regression. It is then used during stage 2 (Sec. 3.2) as an auxiliary stream to provide task features.

We use arbitrary text prompts to identify each task,  $[\text{prompt}]_{\tau} \in \{\text{"normal"}, \text{"depth"}, \dots\}$ . Task prompts are passed through a CLIP text encoder to retrieve their corresponding task tokens:  $c_{\tau} = \text{CLIP}([\text{prompt}]_{\tau})$ . We inject these embeddings to condition the models in Sec. 3.1 and Sec. 3.2.

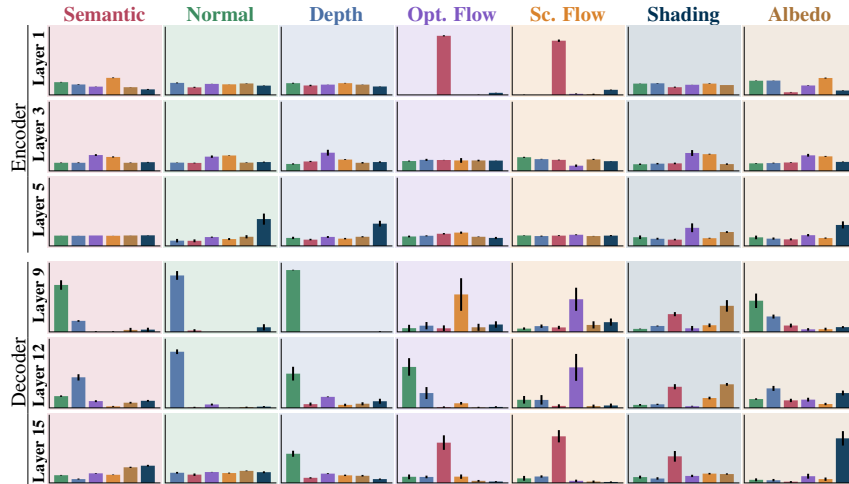


Figure 9: **Task attention scores in the U-Net** ( $U_{\phi,T}$ ) (last layer of each encoder/decoder block shown). Attention becomes more peaky in deeper layers and highlights beneficial cross-task relationships.

### A.3 Training details

For our method, the single stream UNet  $U_{\theta}$  is initialized with weights from Stable Diffusion v2 [50] and trained for 20,000 steps (8 hours). The main stream UNet  $U_{\phi}$  trains for another 10,000 steps (12 hours). For both models, we use Adam optimizer [30] with a learning rate of  $1.0e-4$  and employ an effective batch size of 32 with two gradient accumulation steps on a single H100 GPU.

For adapted baselines, we use the appropriate losses on the added tasks. Considering tasks are mixed inside a mini-batch, we sample them as uniformly as possible across datasets. We use the same augmentations and image resolutions as for training StableMTL. For DiffusionMTL\*, we change the ResNet-50 backbone to the stronger ResNet-101 [26]. In JTR\*, the joint task space and alignment losses are expanded to account for the additional tasks.

### A.4 Evaluation datasets

For **depth** estimation, we evaluate on the KITTI Eigen test split [20, 16] (652 urban images with sparse LiDAR depth) and the DIODE validation split [58] (325 indoor and 446 outdoor LiDAR depth maps); this DIODE split is also utilized for evaluating surface **normal** estimation. For **semantic** segmentation, evaluation is on the Cityscapes validation set [15] (500 images, as test labels are withheld). **Optical Flow** and **scene flow** performance is reported on 200 training images from the KITTI Flow 2025 benchmark [42] (test split is hidden) with semi-automatically established ground truth. Finally, for **shading** and **albedo**, we use the MIT Multi-Illumination dataset’s [45] test set of 750 samples, with ground-truth provided by MIDIntrinsics [9]. For qualitative evaluation, we also employ six additional real-world datasets spanning diverse domains [65, 64, 56, 23, 67, 48].

### A.5 Visualization of task attention on more layers

Figure 9 illustrates the task attention scores across multiple attention layers of the U-Net ( $U_{\phi,T}$ ), showing scores from the last attention layer in each encoder and decoder block. We observe that attention becomes more "peaky" in deeper layers of the network, while it is more homogeneous in the initial layers. This trend is likely because deeper layers encode richer, higher-level features, containing more task-specific information.

StableMTL demonstrates effective attention allocation between known mutually beneficial task pairs, such as **depth/normal**, **optical flow/scene flow**, and **shading/albedo**. Furthermore, it leverages synergies with other tasks. For instance, **semantic** segmentation appears to benefit from **scene flow/optical flow**, potentially helping in differing dynamic and static classes. Similarly, **normal** and **depth** estimation benefit from lighting information provided by **shading**, as lighting conditions can significantly influence the perception of **depth** and surface **normal**.

### A.6 Task attention without separate projection layers ( $q_t, k_t, v_t$ )

Fig. 10 highlights that sharing projection layers across tasks results in highly repetitive attention score patterns. Such patterns may contribute to a decline in multi-task performance, as shown by the row "w/o separate ( $q_t, k_t, v_t$ )" in Tab. 4.

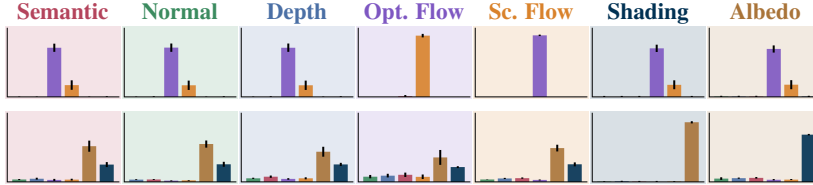


Figure 10: **StableMTL w/o separate** ( $q_t, k_t, v_t$ ). Without separate projection layers ( $q_t, k_t, v_t$ ), the attention pattern is highly repetitive across tasks.

### A.7 More qualitative results

Fig. 11 presents additional qualitative results on real-world data. Notably, StableMTL demonstrates generalization to diverse, multi-task real-world scenarios, even when trained on partially labeled synthetic datasets.

#### B.1 Additional metrics

We present IoU scores for each mapped class on the Cityscapes dataset [15] in Tab. 6, with class mapping details provided in Tab. 9. Overall, StableMTL ranks either first or second on all classes.

Method	road	building	pole	traffic light	traffic sign	vegetation	sky	vehicle	mIoU
Single-task baseline	89.36	61.82	17.13	0.42	3.21	72.75	67.86	72.82	48.17
JTR [46]	96.33	51.48	15.33	0.87	3.22	61.28	77.36	60.16	45.75
JTR* [46]	71.50	0.00	0.00	0.00	0.00	38.69	53.47	0.00	20.46
DiffusionMTL [71]	85.17	29.60	6.64	1.14	5.19	41.05	27.34	44.57	30.09
DiffusionMTL* [71]	95.36	68.26	11.01	4.27	6.40	65.61	48.35	68.15	45.92
StableMTL-S	92.06	67.05	16.76	2.03	6.31	72.53	83.84	80.06	52.57
StableMTL	96.08	74.24	20.72	2.80	12.59	76.58	82.09	81.23	55.79

Table 6: **Per-class Semantic performance.** We report the IoU per mapped semantic class as well as the average IoU (mIoU), detailed in Tab. 9, on Cityscapes.

For **depth** evaluation on KITTI [20] and DIODE [58], additional depth metrics are reported in Tab. 7; these include the following commonly used metrics [16]: absolute relative error (Abs Rel), squared relative error (Sq Rel), root mean squared error (RMSE), mean  $\log_{10}$  error (RMSE log), and threshold accuracies ( $\delta_1, \delta_2, \delta_3$ ). On most of these metrics, StableMTL surpasses all MTL baselines, only performing below the single-stream model StableMTL-S on one metric in one dataset.

We also report, in Tab. 8, metrics for **shading** and **albedo** on the MID dataset [45] following [9]: structural similarity index (SSIM) [62], local mean squared error (LMSE), and root mean squared error (RMSE). These results show our method outperforms all other MTL baselines.

#### B.2 Visualization of task-specific outputs

We detail here the visualization for each task. **Semantic** segmentation maps employ the Cityscapes color scheme (see Tab. 9). For **optical flow**  $\mathbf{v}(u, v) = (v_x, v_y)$ , we adopt the HSV color encoding from [5], where the lateral flow vector's  $(v_x, v_y)$  angle  $\text{atan2}(-v_y, -v_x)$  determines hue and its magnitude  $\|(v_x, v_y)\|_2$  defines saturation, as illustrated in Fig. 12a. Similarly, **Scene Flow**  $\mathbf{v}(u, v) = (v_x, v_y, v_z)$  utilizes an HSV representation (cf. Fig. 12b): its lateral component  $(v_x, v_y)$  determines hue (angle:  $\text{atan2}(-v_y, -v_x)$ ) and saturation (magnitude:  $\|(v_x, v_y)\|_2$ ), while the depth flow component  $v_z$  is inversely mapped to value (brightness), with image-specific scaling applied to

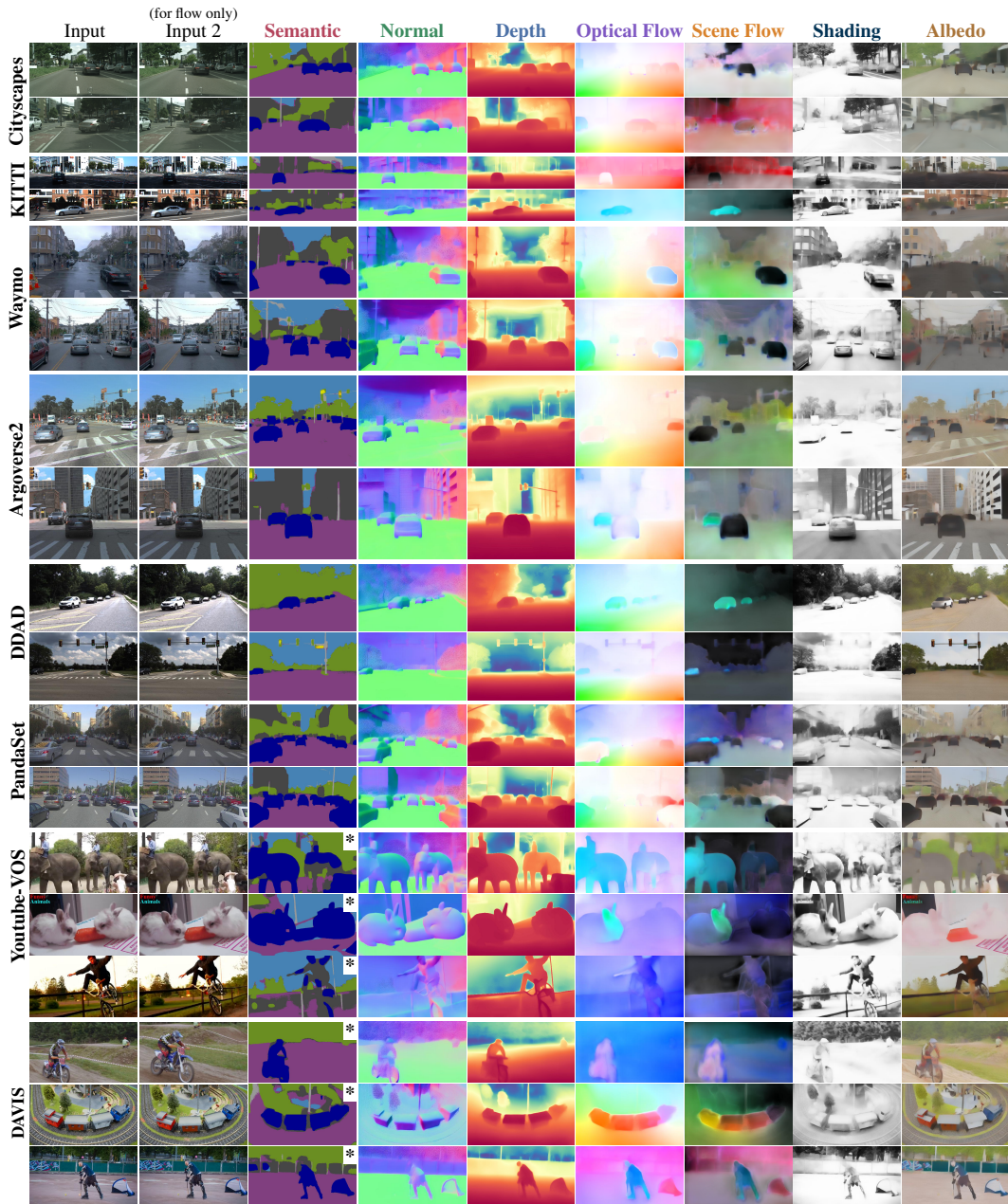


Figure 11: **Additional qualitative results on real-world data.** Despite being trained on partially annotated synthetic datasets, StableMTL demonstrates generalization to multi-task real-world scenarios. \* Note that **semantic** is trained on driving classes and is not expected to generalize to unseen classes.

both the magnitude and  $v_z$ . For **normal** visualization, surface normal XYZ coordinates are directly mapped to RGB space. We predict outward-facing surface normals in OpenCV coordinate system following [4]. **Depth** visualization involves mapping scale-invariant depth values to the spectral color map before display. Finally, **shading** and **albedo** are directly visualized as grayscale and RGB images, respectively.

### B.3 Semantic class mapping

To allow evaluation of **semantic** on the Cityscapes dataset, our model is trained using only a subset of 8 classes, following the VKITTI 2 $\rightarrow$ Cityscapes class mapping from [37], detailed in Tab. 9.

Method	KITTI							DIODE						
	Abs Rel↓	Sq Rel↓	RMSE↓	RMSE log↓	$\delta 1\uparrow$	$\delta 2\uparrow$	$\delta 3\uparrow$	Abs Rel↓	Sq Rel↓	RMSE↓	RMSE log↓	$\delta 1\uparrow$	$\delta 2\uparrow$	$\delta 3\uparrow$
Single-task baseline	14.21	0.7319	4.1734	0.2014	81.19	96.52	99.16	32.56	3.9233	3.9632	0.3163	73.72	87.72	93.11
JTR [46]	26.39	1.7532	6.1357	0.2852	64.60	88.30	95.86	66.39	8.1448	8.4119	0.5482	42.26	67.66	81.59
JTR* [46]	39.27	4.0532	9.1290	0.4301	42.99	73.19	88.00	73.14	9.2842	8.9962	0.5852	40.31	64.24	78.10
DiffusionMTL [71]	21.10	1.4998	5.8491	0.2715	68.11	89.87	96.80	45.19	4.6659	4.9657	0.4106	56.93	78.91	88.56
DiffusionMTL* [71]	24.83	1.8492	6.4705	0.3518	58.77	86.54	95.59	58.17	7.2017	7.6032	0.5166	49.57	73.62	84.55
StableMTL-S	15.64	0.8268	4.3713	0.2499	77.62	95.52	98.72	33.36	3.9504	4.0281	0.3227	73.42	87.17	92.62
StableMTL	14.98	0.8224	4.3707	0.2170	79.43	95.94	98.87	33.03	3.9516	4.0073	0.3192	73.72	87.45	92.89

Table 7: **Additional depth metrics.** In all but one metric, StableMTL ranks first on both KITTI [20] and DIODE [58].

Method	Shading			Albedo		
	RMSE↓	SSIM↑	LMSE↓	RMSE↓	SSIM↑	LMSE↓
Single-task baseline	0.2551	0.4277	0.0426	0.2145	0.6067	0.0505
JTR* [46]	0.3030	0.1843	0.0530	0.3567	0.3102	0.0994
DiffusionMTL* [71]	0.3064	0.3142	0.0487	0.3660	0.3606	0.1620
StableMTL-S	0.2311	0.4449	0.0363	0.2077	0.6151	0.0496
StableMTL	0.2346	0.4424	0.0366	0.2016	0.6199	0.0477

Table 8: **Additional shading and albedo metrics.** On MIDIntrinsics [45], StableMTL ranks either first or second; it is only surpassed by our single stream variant StableMTL-S.

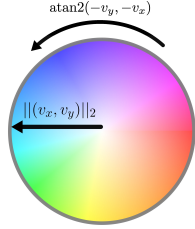
#### B.4 Image resolutions for training and evaluation

We train the model on datasets using the following pixel resolutions,  $\text{height} \times \text{width}$ :

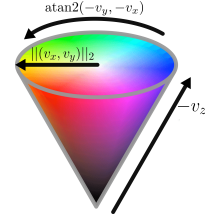
- Hypersim (288×384),
- FlyingThings3D (268×480),
- VKITTI2 (187×621).

For evaluation, we use the following resolutions:

- Cityscapes (256×512),
- DIODE (384×512),
- KITTI (176×608),
- MIDIntrinsics (256×384).



(a) **Optical Flow** color mapping.



(b) **Scene Flow** color mapping.

Figure 12: **Flow color mappings.** We visualize the mapping used to visualize (a) **optical flow** and (b) **scene flow**.

VKITTI 2	ours	Cityscapes	ours	Color
terrain	<i>ignore</i>	road	road	■
sky	sky	sidewalk	<i>ignore</i>	■
tree	vegetation	building	building	■
vegetation	vegetation	wall	vegetation	■
building	building	fence	<i>ignore</i>	■
road	road	pole	pole	■
guardrail	<i>ignore</i>	light	light	■
sign	sign	sign	sign	■
light	light	vegetation	vegetation	■
pole	pole	sky	sky	■
misc	<i>ignore</i>	person	<i>ignore</i>	■
truck	vehicle	rider	<i>ignore</i>	■
car	vehicle	car	vehicle	■
van	vehicle	bus	vehicle	■
		motorbike	<i>ignore</i>	■
		bike	<i>ignore</i>	■

Table 9: **Classes used for training.** We use a common set of 8 classes (ours), mapping together semantically similar classes of VKITTI 2, which enables proper evaluation of our model on Cityscapes.

---

# Formatting Instructions For NeurIPS 2025

---

## Anonymous Author(s)

Affiliation

Address

email

## Abstract

1 The abstract paragraph should be indented  $\frac{1}{2}$  inch (3 picas) on both the left- and  
2 right-hand margins. Use 10 point type, with a vertical spacing (leading) of 11 points.  
3 The word **Abstract** must be centered, bold, and in point size 12. Two line spaces  
4 precede the abstract. The abstract must be limited to one paragraph.

## 5 1 Submission of papers to NeurIPS 2025

6 Please read the instructions below carefully and follow them faithfully.

### 7 1.1 Style

8 Papers to be submitted to NeurIPS 2025 must be prepared according to the instructions presented  
9 here. Papers may only be up to **nine** pages long, including figures. Additional pages *containing*  
10 *references, checklist, and the optional technical appendices* do not count as content pages. Papers  
11 that exceed the page limit will not be reviewed, or in any other way considered for presentation at the  
12 conference.

13 The margins in 2025 are the same as those in previous years.

14 Authors are required to use the NeurIPS L<sup>A</sup>T<sub>E</sub>X style files obtainable at the NeurIPS website as  
15 indicated below. Please make sure you use the current files and not previous versions. Tweaking the  
16 style files may be grounds for rejection.

### 17 1.2 Retrieval of style files

18 The style files for NeurIPS and other conference information are available on the website at

19 <https://neurips.cc>

20 The file `neurips_2025.pdf` contains these instructions and illustrates the various formatting re-  
21 quirements your NeurIPS paper must satisfy.

22 The only supported style file for NeurIPS 2025 is `neurips_2025.sty`, rewritten for L<sup>A</sup>T<sub>E</sub>X 2<sub>ε</sub>.  
23 **Previous style files for L<sup>A</sup>T<sub>E</sub>X 2.09, Microsoft Word, and RTF are no longer supported!**

24 The L<sup>A</sup>T<sub>E</sub>X style file contains three optional arguments: `final`, which creates a camera-ready copy,  
25 `preprint`, which creates a preprint for submission to, e.g., arXiv, and `nonatbib`, which will not  
26 load the `natbib` package for you in case of package clash.

27 **Preprint option** If you wish to post a preprint of your work online, e.g., on arXiv, using the  
28 NeurIPS style, please use the `preprint` option. This will create a nonanonymized version of your  
29 work with the text “Preprint. Work in progress.” in the footer. This version may be distributed as you

30 see fit, as long as you do not say which conference it was submitted to. Please **do not** use the `final`  
31 option, which should **only** be used for papers accepted to NeurIPS.

32 At submission time, please omit the `final` and `preprint` options. This will anonymize your  
33 submission and add line numbers to aid review. Please do *not* refer to these line numbers in your  
34 paper as they will be removed during generation of camera-ready copies.

35 The file `neurips_2025.tex` may be used as a “shell” for writing your paper. All you have to do is  
36 replace the author, title, abstract, and text of the paper with your own.

37 The formatting instructions contained in these style files are summarized in Sections 2, 3, and 4  
38 below.

## 39 **2 General formatting instructions**

40 The text must be confined within a rectangle 5.5 inches (33 picas) wide and 9 inches (54 picas) long.  
41 The left margin is 1.5 inch (9 picas). Use 10 point type with a vertical spacing (leading) of 11 points.  
42 Times New Roman is the preferred typeface throughout, and will be selected for you by default.  
43 Paragraphs are separated by  $\frac{1}{2}$  line space (5.5 points), with no indentation.

44 The paper title should be 17 point, initial caps/lower case, bold, centered between two horizontal  
45 rules. The top rule should be 4 points thick and the bottom rule should be 1 point thick. Allow  $\frac{1}{4}$  inch  
46 space above and below the title to rules. All pages should start at 1 inch (6 picas) from the top of the  
47 page.

48 For the final version, authors’ names are set in boldface, and each name is centered above the  
49 corresponding address. The lead author’s name is to be listed first (left-most), and the co-authors’  
50 names (if different address) are set to follow. If there is only one co-author, list both author and  
51 co-author side by side.

52 Please pay special attention to the instructions in Section 4 regarding figures, tables, acknowledgments,  
53 and references.

## 54 **3 Headings: first level**

55 All headings should be lower case (except for first word and proper nouns), flush left, and bold.

56 First-level headings should be in 12-point type.

### 57 **3.1 Headings: second level**

58 Second-level headings should be in 10-point type.

#### 59 **3.1.1 Headings: third level**

60 Third-level headings should be in 10-point type.

61 **Paragraphs** There is also a `\paragraph` command available, which sets the heading in bold, flush  
62 left, and inline with the text, with the heading followed by 1 em of space.

## 63 **4 Citations, figures, tables, references**

64 These instructions apply to everyone.

### 65 **4.1 Citations within the text**

66 The `natbib` package will be loaded for you by default. Citations may be author/year or numeric, as  
67 long as you maintain internal consistency. As to the format of the references themselves, any style is  
68 acceptable as long as it is used consistently.

69 The documentation for `natbib` may be found at

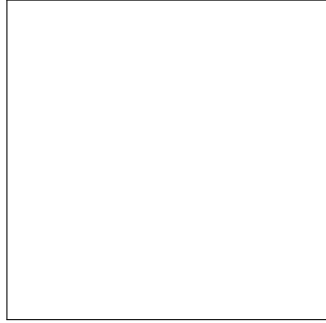


Figure 1: Sample figure caption.

70 `http://mirrors.ctan.org/macros/latex/contrib/natbib/natnotes.pdf`

71 Of note is the command `\citet`, which produces citations appropriate for use in inline text. For  
72 example,

73 `\citet{hasselmo}` investigated\dots

74 produces

75 Hasselmo, et al. (1995) investigated...

76 If you wish to load the `natbib` package with options, you may add the following before loading the  
77 `neurips_2025` package:

78 `\PassOptionsToPackage{options}{natbib}`

79 If `natbib` clashes with another package you load, you can add the optional argument `nonatbib`  
80 when loading the style file:

81 `\usepackage[nonatbib]{neurips_2025}`

82 As submission is double blind, refer to your own published work in the third person. That is, use “In  
83 the previous work of Jones et al. [4],” not “In our previous work [4].” If you cite your other papers  
84 that are not widely available (e.g., a journal paper under review), use anonymous author names in the  
85 citation, e.g., an author of the form “A. Anonymous” and include a copy of the anonymized paper in  
86 the supplementary material.

## 87 4.2 Footnotes

88 Footnotes should be used sparingly. If you do require a footnote, indicate footnotes with a number<sup>1</sup>  
89 in the text. Place the footnotes at the bottom of the page on which they appear. Precede the footnote  
90 with a horizontal rule of 2 inches (12 picas).

91 Note that footnotes are properly typeset *after* punctuation marks.<sup>2</sup>

## 92 4.3 Figures

93 All artwork must be neat, clean, and legible. Lines should be dark enough for purposes of reproduction.  
94 The figure number and caption always appear after the figure. Place one line space before the figure  
95 caption and one line space after the figure. The figure caption should be lower case (except for first  
96 word and proper nouns); figures are numbered consecutively.

97 You may use color figures. However, it is best for the figure captions and the paper body to be legible  
98 if the paper is printed in either black/white or in color.

---

<sup>1</sup>Sample of the first footnote.

<sup>2</sup>As in this example.

Table 1: Sample table title

Part		
Name	Description	Size ( $\mu\text{m}$ )
Dendrite	Input terminal	$\sim 100$
Axon	Output terminal	$\sim 10$
Soma	Cell body	up to $10^6$

99 **4.4 Tables**

100 All tables must be centered, neat, clean and legible. The table number and title always appear before  
101 the table. See Table 1.

102 Place one line space before the table title, one line space after the table title, and one line space after  
103 the table. The table title must be lower case (except for first word and proper nouns); tables are  
104 numbered consecutively.

105 Note that publication-quality tables *do not contain vertical rules*. We strongly suggest the use of the  
106 `booktabs` package, which allows for typesetting high-quality, professional tables:

107 `https://www.ctan.org/pkg/booktabs`

108 This package was used to typeset Table 1.

109 **4.5 Math**

110 Note that display math in bare TeX commands will not create correct line numbers for sub-  
111 mission. Please use LaTeX (or AMSTeX) commands for unnumbered display math. (You  
112 really shouldn't be using  $\$$  anyway; see <https://tex.stackexchange.com/questions/503/why-is-preferable-to> and <https://tex.stackexchange.com/questions/40492/what-are-the-differences-between-align-equation-and-displaymath> for more infor-  
113 mation.)  
114 mation.)  
115 mation.)

116 **4.6 Final instructions**

117 Do not change any aspects of the formatting parameters in the style files. In particular, do not modify  
118 the width or length of the rectangle the text should fit into, and do not change font sizes (except  
119 perhaps in the **References** section; see below). Please note that pages should be numbered.

120 **5 Preparing PDF files**

121 Please prepare submission files with paper size "US Letter," and not, for example, "A4."

122 Fonts were the main cause of problems in the past years. Your PDF file must only contain Type 1 or  
123 Embedded TrueType fonts. Here are a few instructions to achieve this.

- 124 • You should directly generate PDF files using `pdflatex`.
- 125 • You can check which fonts a PDF files uses. In Acrobat Reader, select the menu  
126 Files>Document Properties>Fonts and select Show All Fonts. You can also use the program  
127 `pdf-fonts` which comes with `xpdf` and is available out-of-the-box on most Linux machines.
- 128 • `xfig` "patterned" shapes are implemented with bitmap fonts. Use "solid" shapes instead.
- 129 • The `\bbold` package almost always uses bitmap fonts. You should use the equivalent AMS  
130 Fonts:

131 `\usepackage{amsfonts}`

132 followed by, e.g., `\mathbb{R}`, `\mathbb{N}`, or `\mathbb{C}` for  $\mathbb{R}$ ,  $\mathbb{N}$  or  $\mathbb{C}$ . You can also  
133 use the following workaround for reals, natural and complex:

```
134 \newcommand{\RR}{\mathbb{R}} %real numbers
135 \newcommand{\Nat}{\mathbb{N}} %natural numbers
136 \newcommand{\CC}{\mathbb{C}} %complex numbers
```

137 Note that `amsfonts` is automatically loaded by the `amssymb` package.

138 If your file contains type 3 fonts or non embedded TrueType fonts, we will ask you to fix it.

## 139 5.1 Margins in L<sup>A</sup>T<sub>E</sub>X

140 Most of the margin problems come from figures positioned by hand using `\special` or other  
141 commands. We suggest using the command `\includegraphics` from the `graphicx` package.  
142 Always specify the figure width as a multiple of the line width as in the example below:

```
143 \usepackage[pdftex]{graphicx} ...
144 \includegraphics[width=0.8\linewidth]{myfile.pdf}
```

145 See Section 4.4 in the graphics bundle documentation ([http://mirrors.ctan.org/macros/](http://mirrors.ctan.org/macros/latex/required/graphics/grfguide.pdf)  
146 [latex/required/graphics/grfguide.pdf](http://mirrors.ctan.org/macros/latex/required/graphics/grfguide.pdf))

147 A number of width problems arise when L<sup>A</sup>T<sub>E</sub>X cannot properly hyphenate a line. Please give LaTeX  
148 hyphenation hints using the `\-` command when necessary.

## 149 References

150 References follow the acknowledgments in the camera-ready paper. Use unnumbered first-level  
151 heading for the references. Any choice of citation style is acceptable as long as you are consistent. It  
152 is permissible to reduce the font size to `small` (9 point) when listing the references. Note that the  
153 Reference section does not count towards the page limit.

154 [1] Alexander, J.A. & Mozer, M.C. (1995) Template-based algorithms for connectionist rule extraction. In  
155 G. Tesauro, D.S. Touretzky and T.K. Leen (eds.), *Advances in Neural Information Processing Systems 7*, pp.  
156 609–616. Cambridge, MA: MIT Press.

157 [2] Bower, J.M. & Beeman, D. (1995) *The Book of GENESIS: Exploring Realistic Neural Models with the*  
158 *GENeral NEural Simulation System*. New York: TELOS/Springer-Verlag.

159 [3] Hasselmo, M.E., Schnell, E. & Barkai, E. (1995) Dynamics of learning and recall at excitatory recurrent  
160 synapses and cholinergic modulation in rat hippocampal region CA3. *Journal of Neuroscience* **15**(7):5249-5262.

## 161 A Technical Appendices and Supplementary Material

162 Technical appendices with additional results, figures, graphs and proofs may be submitted with  
163 the paper submission before the full submission deadline (see above), or as a separate PDF in the  
164 ZIP file below before the supplementary material deadline. There is no page limit for the technical  
165 appendices.

166 **NeurIPS Paper Checklist**

167 The checklist is designed to encourage best practices for responsible machine learning research,  
168 addressing issues of reproducibility, transparency, research ethics, and societal impact. Do not remove  
169 the checklist: **The papers not including the checklist will be desk rejected.** The checklist should  
170 follow the references and follow the (optional) supplemental material. The checklist does NOT count  
171 towards the page limit.

172 Please read the checklist guidelines carefully for information on how to answer these questions. For  
173 each question in the checklist:

- 174 • You should answer [Yes], [No], or [NA].
- 175 • [NA] means either that the question is Not Applicable for that particular paper or the  
176 relevant information is Not Available.
- 177 • Please provide a short (1–2 sentence) justification right after your answer (even for NA).

178 **The checklist answers are an integral part of your paper submission.** They are visible to the  
179 reviewers, area chairs, senior area chairs, and ethics reviewers. You will be asked to also include it  
180 (after eventual revisions) with the final version of your paper, and its final version will be published  
181 with the paper.

182 The reviewers of your paper will be asked to use the checklist as one of the factors in their evaluation.  
183 While "[Yes]" is generally preferable to "[No]", it is perfectly acceptable to answer "[No]" provided a  
184 proper justification is given (e.g., "error bars are not reported because it would be too computationally  
185 expensive" or "we were unable to find the license for the dataset we used"). In general, answering  
186 "[No]" or "[NA]" is not grounds for rejection. While the questions are phrased in a binary way, we  
187 acknowledge that the true answer is often more nuanced, so please just use your best judgment and  
188 write a justification to elaborate. All supporting evidence can appear either in the main paper or the  
189 supplemental material, provided in appendix. If you answer [Yes] to a question, in the justification  
190 please point to the section(s) where related material for the question can be found.

191 IMPORTANT, please:

- 192 • **Delete this instruction block, but keep the section heading “NeurIPS Paper Checklist”,**
- 193 • **Keep the checklist subsection headings, questions/answers and guidelines below.**
- 194 • **Do not modify the questions and only use the provided macros for your answers.**

195 **1. Claims**

196 Question: Do the main claims made in the abstract and introduction accurately reflect the  
197 paper’s contributions and scope?

198 Answer: **[TODO]**

199 Justification: **[TODO]**

200 Guidelines:

- 201 • The answer NA means that the abstract and introduction do not include the claims  
202 made in the paper.
- 203 • The abstract and/or introduction should clearly state the claims made, including the  
204 contributions made in the paper and important assumptions and limitations. A No or  
205 NA answer to this question will not be perceived well by the reviewers.
- 206 • The claims made should match theoretical and experimental results, and reflect how  
207 much the results can be expected to generalize to other settings.
- 208 • It is fine to include aspirational goals as motivation as long as it is clear that these goals  
209 are not attained by the paper.

210 **2. Limitations**

211 Question: Does the paper discuss the limitations of the work performed by the authors?

212 Answer: **[TODO]**

213 Justification: **[TODO]**

214  
215  
216  
217  
218  
219  
220  
221  
222  
223  
224  
225  
226  
227  
228  
229  
230  
231  
232  
233  
234  
235  
236  
237  
238  
239  
240  
241  
242  
243  
244  
245  
246  
247  
248  
249  
250  
251  
252  
253  
254  
255  
256  
257  
258  
259  
260  
261  
262  
263  
264

Guidelines:

- The answer NA means that the paper has no limitation while the answer No means that the paper has limitations, but those are not discussed in the paper.
- The authors are encouraged to create a separate "Limitations" section in their paper.
- The paper should point out any strong assumptions and how robust the results are to violations of these assumptions (e.g., independence assumptions, noiseless settings, model well-specification, asymptotic approximations only holding locally). The authors should reflect on how these assumptions might be violated in practice and what the implications would be.
- The authors should reflect on the scope of the claims made, e.g., if the approach was only tested on a few datasets or with a few runs. In general, empirical results often depend on implicit assumptions, which should be articulated.
- The authors should reflect on the factors that influence the performance of the approach. For example, a facial recognition algorithm may perform poorly when image resolution is low or images are taken in low lighting. Or a speech-to-text system might not be used reliably to provide closed captions for online lectures because it fails to handle technical jargon.
- The authors should discuss the computational efficiency of the proposed algorithms and how they scale with dataset size.
- If applicable, the authors should discuss possible limitations of their approach to address problems of privacy and fairness.
- While the authors might fear that complete honesty about limitations might be used by reviewers as grounds for rejection, a worse outcome might be that reviewers discover limitations that aren't acknowledged in the paper. The authors should use their best judgment and recognize that individual actions in favor of transparency play an important role in developing norms that preserve the integrity of the community. Reviewers will be specifically instructed to not penalize honesty concerning limitations.

**3. Theory assumptions and proofs**

Question: For each theoretical result, does the paper provide the full set of assumptions and a complete (and correct) proof?

Answer: **[TODO]**

Justification: **[TODO]**

Guidelines:

- The answer NA means that the paper does not include theoretical results.
- All the theorems, formulas, and proofs in the paper should be numbered and cross-referenced.
- All assumptions should be clearly stated or referenced in the statement of any theorems.
- The proofs can either appear in the main paper or the supplemental material, but if they appear in the supplemental material, the authors are encouraged to provide a short proof sketch to provide intuition.
- Inversely, any informal proof provided in the core of the paper should be complemented by formal proofs provided in appendix or supplemental material.
- Theorems and Lemmas that the proof relies upon should be properly referenced.

**4. Experimental result reproducibility**

Question: Does the paper fully disclose all the information needed to reproduce the main experimental results of the paper to the extent that it affects the main claims and/or conclusions of the paper (regardless of whether the code and data are provided or not)?

Answer: **[TODO]**

Justification: **[TODO]**

Guidelines:

- The answer NA means that the paper does not include experiments.

- 265 • If the paper includes experiments, a No answer to this question will not be perceived  
266 well by the reviewers: Making the paper reproducible is important, regardless of  
267 whether the code and data are provided or not.
- 268 • If the contribution is a dataset and/or model, the authors should describe the steps taken  
269 to make their results reproducible or verifiable.
- 270 • Depending on the contribution, reproducibility can be accomplished in various ways.  
271 For example, if the contribution is a novel architecture, describing the architecture fully  
272 might suffice, or if the contribution is a specific model and empirical evaluation, it may  
273 be necessary to either make it possible for others to replicate the model with the same  
274 dataset, or provide access to the model. In general, releasing code and data is often  
275 one good way to accomplish this, but reproducibility can also be provided via detailed  
276 instructions for how to replicate the results, access to a hosted model (e.g., in the case  
277 of a large language model), releasing of a model checkpoint, or other means that are  
278 appropriate to the research performed.
- 279 • While NeurIPS does not require releasing code, the conference does require all submis-  
280 sions to provide some reasonable avenue for reproducibility, which may depend on the  
281 nature of the contribution. For example
  - 282 (a) If the contribution is primarily a new algorithm, the paper should make it clear how  
283 to reproduce that algorithm.
  - 284 (b) If the contribution is primarily a new model architecture, the paper should describe  
285 the architecture clearly and fully.
  - 286 (c) If the contribution is a new model (e.g., a large language model), then there should  
287 either be a way to access this model for reproducing the results or a way to reproduce  
288 the model (e.g., with an open-source dataset or instructions for how to construct  
289 the dataset).
  - 290 (d) We recognize that reproducibility may be tricky in some cases, in which case  
291 authors are welcome to describe the particular way they provide for reproducibility.  
292 In the case of closed-source models, it may be that access to the model is limited in  
293 some way (e.g., to registered users), but it should be possible for other researchers  
294 to have some path to reproducing or verifying the results.

## 295 5. Open access to data and code

296 Question: Does the paper provide open access to the data and code, with sufficient instruc-  
297 tions to faithfully reproduce the main experimental results, as described in supplemental  
298 material?

299 Answer: **[TODO]**

300 Justification: **[TODO]**

301 Guidelines:

- 302 • The answer NA means that paper does not include experiments requiring code.
- 303 • Please see the NeurIPS code and data submission guidelines ([https://nips.cc/  
304 public/guides/CodeSubmissionPolicy](https://nips.cc/public/guides/CodeSubmissionPolicy)) for more details.
- 305 • While we encourage the release of code and data, we understand that this might not be  
306 possible, so “No” is an acceptable answer. Papers cannot be rejected simply for not  
307 including code, unless this is central to the contribution (e.g., for a new open-source  
308 benchmark).
- 309 • The instructions should contain the exact command and environment needed to run to  
310 reproduce the results. See the NeurIPS code and data submission guidelines ([https://  
311 nips.cc/public/guides/CodeSubmissionPolicy](https://nips.cc/public/guides/CodeSubmissionPolicy)) for more details.
- 312 • The authors should provide instructions on data access and preparation, including how  
313 to access the raw data, preprocessed data, intermediate data, and generated data, etc.
- 314 • The authors should provide scripts to reproduce all experimental results for the new  
315 proposed method and baselines. If only a subset of experiments are reproducible, they  
316 should state which ones are omitted from the script and why.
- 317 • At submission time, to preserve anonymity, the authors should release anonymized  
318 versions (if applicable).

- 319                   • Providing as much information as possible in supplemental material (appended to the  
320 paper) is recommended, but including URLs to data and code is permitted.

321 **6. Experimental setting/details**

322 Question: Does the paper specify all the training and test details (e.g., data splits, hyper-  
323 parameters, how they were chosen, type of optimizer, etc.) necessary to understand the  
324 results?

325 Answer: **[TODO]**

326 Justification: **[TODO]**

327 Guidelines:

- 328 • The answer NA means that the paper does not include experiments.
- 329 • The experimental setting should be presented in the core of the paper to a level of detail  
330 that is necessary to appreciate the results and make sense of them.
- 331 • The full details can be provided either with the code, in appendix, or as supplemental  
332 material.

333 **7. Experiment statistical significance**

334 Question: Does the paper report error bars suitably and correctly defined or other appropriate  
335 information about the statistical significance of the experiments?

336 Answer: **[TODO]**

337 Justification: **[TODO]**

338 Guidelines:

- 339 • The answer NA means that the paper does not include experiments.
- 340 • The authors should answer "Yes" if the results are accompanied by error bars, confi-  
341 dence intervals, or statistical significance tests, at least for the experiments that support  
342 the main claims of the paper.
- 343 • The factors of variability that the error bars are capturing should be clearly stated (for  
344 example, train/test split, initialization, random drawing of some parameter, or overall  
345 run with given experimental conditions).
- 346 • The method for calculating the error bars should be explained (closed form formula,  
347 call to a library function, bootstrap, etc.)
- 348 • The assumptions made should be given (e.g., Normally distributed errors).
- 349 • It should be clear whether the error bar is the standard deviation or the standard error  
350 of the mean.
- 351 • It is OK to report 1-sigma error bars, but one should state it. The authors should  
352 preferably report a 2-sigma error bar than state that they have a 96% CI, if the hypothesis  
353 of Normality of errors is not verified.
- 354 • For asymmetric distributions, the authors should be careful not to show in tables or  
355 figures symmetric error bars that would yield results that are out of range (e.g. negative  
356 error rates).
- 357 • If error bars are reported in tables or plots, The authors should explain in the text how  
358 they were calculated and reference the corresponding figures or tables in the text.

359 **8. Experiments compute resources**

360 Question: For each experiment, does the paper provide sufficient information on the com-  
361 puter resources (type of compute workers, memory, time of execution) needed to reproduce  
362 the experiments?

363 Answer: **[TODO]**

364 Justification: **[TODO]**

365 Guidelines:

- 366 • The answer NA means that the paper does not include experiments.
- 367 • The paper should indicate the type of compute workers CPU or GPU, internal cluster,  
368 or cloud provider, including relevant memory and storage.

- 369
- The paper should provide the amount of compute required for each of the individual experimental runs as well as estimate the total compute.
- 370
- The paper should disclose whether the full research project required more compute than the experiments reported in the paper (e.g., preliminary or failed experiments that didn't make it into the paper).
- 371
- 372
- 373

## 374 9. Code of ethics

375 Question: Does the research conducted in the paper conform, in every respect, with the  
376 NeurIPS Code of Ethics <https://neurips.cc/public/EthicsGuidelines?>

377 Answer: **[TODO]**

378 Justification: **[TODO]**

379 Guidelines:

- The answer NA means that the authors have not reviewed the NeurIPS Code of Ethics.
  - If the authors answer No, they should explain the special circumstances that require a deviation from the Code of Ethics.
  - The authors should make sure to preserve anonymity (e.g., if there is a special consideration due to laws or regulations in their jurisdiction).
- 380
- 381
- 382
- 383
- 384

## 385 10. Broader impacts

386 Question: Does the paper discuss both potential positive societal impacts and negative  
387 societal impacts of the work performed?

388 Answer: **[TODO]**

389 Justification: **[TODO]**

390 Guidelines:

- The answer NA means that there is no societal impact of the work performed.
  - If the authors answer NA or No, they should explain why their work has no societal impact or why the paper does not address societal impact.
  - Examples of negative societal impacts include potential malicious or unintended uses (e.g., disinformation, generating fake profiles, surveillance), fairness considerations (e.g., deployment of technologies that could make decisions that unfairly impact specific groups), privacy considerations, and security considerations.
  - The conference expects that many papers will be foundational research and not tied to particular applications, let alone deployments. However, if there is a direct path to any negative applications, the authors should point it out. For example, it is legitimate to point out that an improvement in the quality of generative models could be used to generate deepfakes for disinformation. On the other hand, it is not needed to point out that a generic algorithm for optimizing neural networks could enable people to train models that generate Deepfakes faster.
  - The authors should consider possible harms that could arise when the technology is being used as intended and functioning correctly, harms that could arise when the technology is being used as intended but gives incorrect results, and harms following from (intentional or unintentional) misuse of the technology.
  - If there are negative societal impacts, the authors could also discuss possible mitigation strategies (e.g., gated release of models, providing defenses in addition to attacks, mechanisms for monitoring misuse, mechanisms to monitor how a system learns from feedback over time, improving the efficiency and accessibility of ML).
- 391
- 392
- 393
- 394
- 395
- 396
- 397
- 398
- 399
- 400
- 401
- 402
- 403
- 404
- 405
- 406
- 407
- 408
- 409
- 410
- 411
- 412

## 413 11. Safeguards

414 Question: Does the paper describe safeguards that have been put in place for responsible  
415 release of data or models that have a high risk for misuse (e.g., pretrained language models,  
416 image generators, or scraped datasets)?

417 Answer: **[TODO]**

418 Justification: **[TODO]**

419 Guidelines:

- The answer NA means that the paper poses no such risks.
- 420

- 421 • Released models that have a high risk for misuse or dual-use should be released with  
422 necessary safeguards to allow for controlled use of the model, for example by requiring  
423 that users adhere to usage guidelines or restrictions to access the model or implementing  
424 safety filters.
- 425 • Datasets that have been scraped from the Internet could pose safety risks. The authors  
426 should describe how they avoided releasing unsafe images.
- 427 • We recognize that providing effective safeguards is challenging, and many papers do  
428 not require this, but we encourage authors to take this into account and make a best  
429 faith effort.

## 430 12. Licenses for existing assets

431 Question: Are the creators or original owners of assets (e.g., code, data, models), used in  
432 the paper, properly credited and are the license and terms of use explicitly mentioned and  
433 properly respected?

434 Answer: **[TODO]**

435 Justification: **[TODO]**

436 Guidelines:

- 437 • The answer NA means that the paper does not use existing assets.
- 438 • The authors should cite the original paper that produced the code package or dataset.
- 439 • The authors should state which version of the asset is used and, if possible, include a  
440 URL.
- 441 • The name of the license (e.g., CC-BY 4.0) should be included for each asset.
- 442 • For scraped data from a particular source (e.g., website), the copyright and terms of  
443 service of that source should be provided.
- 444 • If assets are released, the license, copyright information, and terms of use in the  
445 package should be provided. For popular datasets, `paperswithcode.com/datasets`  
446 has curated licenses for some datasets. Their licensing guide can help determine the  
447 license of a dataset.
- 448 • For existing datasets that are re-packaged, both the original license and the license of  
449 the derived asset (if it has changed) should be provided.
- 450 • If this information is not available online, the authors are encouraged to reach out to  
451 the asset's creators.

## 452 13. New assets

453 Question: Are new assets introduced in the paper well documented and is the documentation  
454 provided alongside the assets?

455 Answer: **[TODO]**

456 Justification: **[TODO]**

457 Guidelines:

- 458 • The answer NA means that the paper does not release new assets.
- 459 • Researchers should communicate the details of the dataset/code/model as part of their  
460 submissions via structured templates. This includes details about training, license,  
461 limitations, etc.
- 462 • The paper should discuss whether and how consent was obtained from people whose  
463 asset is used.
- 464 • At submission time, remember to anonymize your assets (if applicable). You can either  
465 create an anonymized URL or include an anonymized zip file.

## 466 14. Crowdsourcing and research with human subjects

467 Question: For crowdsourcing experiments and research with human subjects, does the paper  
468 include the full text of instructions given to participants and screenshots, if applicable, as  
469 well as details about compensation (if any)?

470 Answer: **[TODO]**

471 Justification: **[TODO]**

472  
473  
474  
475  
476  
477  
478  
479  
480  
481  
482  
483  
484  
485  
486  
487  
488  
489  
490  
491  
492  
493  
494  
495  
496  
497  
498  
499  
500  
501  
502  
503  
504  
505  
506  
507  
508  
509  
510  
511

Guidelines:

- The answer NA means that the paper does not involve crowdsourcing nor research with human subjects.
- Including this information in the supplemental material is fine, but if the main contribution of the paper involves human subjects, then as much detail as possible should be included in the main paper.
- According to the NeurIPS Code of Ethics, workers involved in data collection, curation, or other labor should be paid at least the minimum wage in the country of the data collector.

**15. Institutional review board (IRB) approvals or equivalent for research with human subjects**

Question: Does the paper describe potential risks incurred by study participants, whether such risks were disclosed to the subjects, and whether Institutional Review Board (IRB) approvals (or an equivalent approval/review based on the requirements of your country or institution) were obtained?

Answer: **[TODO]**

Justification: **[TODO]**

Guidelines:

- The answer NA means that the paper does not involve crowdsourcing nor research with human subjects.
- Depending on the country in which research is conducted, IRB approval (or equivalent) may be required for any human subjects research. If you obtained IRB approval, you should clearly state this in the paper.
- We recognize that the procedures for this may vary significantly between institutions and locations, and we expect authors to adhere to the NeurIPS Code of Ethics and the guidelines for their institution.
- For initial submissions, do not include any information that would break anonymity (if applicable), such as the institution conducting the review.

**16. Declaration of LLM usage**

Question: Does the paper describe the usage of LLMs if it is an important, original, or non-standard component of the core methods in this research? Note that if the LLM is used only for writing, editing, or formatting purposes and does not impact the core methodology, scientific rigorousness, or originality of the research, declaration is not required.

Answer: **[TODO]**

Justification: **[TODO]**

Guidelines:

- The answer NA means that the core method development in this research does not involve LLMs as any important, original, or non-standard components.
- Please refer to our LLM policy (<https://neurips.cc/Conferences/2025/LLM>) for what should or should not be described.